Normal form maps for grazing bifurcations in n-dimensional piecewise-smooth dynamical systems

M. di Bernardo*†, C.J. Budd‡and A.R. Champneys§

July 27, 2000

Abstract

This paper presents a unified framework for performing local analysis of *grazing bifurcations* in n-dimensional piecewise-smooth systems of ODEs. These occur when a periodic orbit has a point of tangency with a smooth $(n-1)$-dimensional boundary dividing distinct regions in phase space where the vector field is smooth. It is shown under quite general circumstances that this leads to a normal-form map that contains to lowest order either a *square-root* or a $(3/2)$-*type singularity* according to whether the vector field is discontinuous or not at the grazing point. In particular, contrary to what has been reported in the literature, *piecewise-linear* local maps do not occur generically.

First, the concept of a grazing bifurcation is carefully defined using appropriate non-degeneracy conditions. Next, complete expressions are derived for calculating the leading-order term in the normal form Poincaré map at a grazing bifurcation point in arbitrary systems, using the concept of a *discontinuity mapping*. Finally, the theory is compared with numerical examples including bilinear oscillators, a relay feedback controller and general third-order systems.

1 Background

Switching and impacting behaviour is found in many devices of relevance in engineering and applied science [Brogliato 1999]. Electronic circuits and vibro-impacting machines, for instance, provide examples of systems whose dynamical behaviour is affected by the occurrence of discontinuous events. These events include the switching of a system component (diode, transistor etc.) or the collision with an external obstacle or wall [Deane & Hamill 1990, Norsworthy, Schreier & Temes 1997, Budd & Dux 1994*a*]. Further examples include suspension bridges, rocking blocks, walking mechanisms, friction oscillators and many others [Peterka 1974, Doole & Hogan 1996, Fossas & Olivar 1996, Hogan 1989, McGeer 1990, Popp, Hinrichs & Oestreich 1995].

Because of their non-smooth nature, these devices are usually modelled by means of appropriate piecewise-smooth sets of ODEs of the form

$$\dot{x} = F(x, t, \mu), \tag{1.1}$$

with $F : \mathbb{R}^{n+m+1} \mapsto \mathbb{R}$ being a piecewise-smooth (PWS) function, t the time variable, $p \in \mathbb{R}^m$ a parameter vector and $x \in \mathbb{R}^n$ the state vector. The phase space of such a general system can be partitioned into finitely many regions associated with different functional forms of the system, separated by smooth $(n-1)$-dimensional boundaries.

Recently, it has been pointed out that even simple switching systems can exhibit a plethora of complicated dynamical regimes. Several dramatic bifurcation scenarios are known including the sudden transition from stable periodic motion to fully developed chaotic behaviour (e.g. [di Bernardo, Feigin, Hogan & Homer

*Department of Engineering Mathematics, University of Bristol BS8 1TR U.K. m.dibernardo@bris.ac.uk
†Corresponding author.
‡School of Mathematical Sciences, University of Bath BA2 7AY U.K. cjb@maths.bath.ac.uk
§Department of Engineering Mathematics, University of Bristol BS8 1TR U.K. a.r.champneys@bris.ac.uk

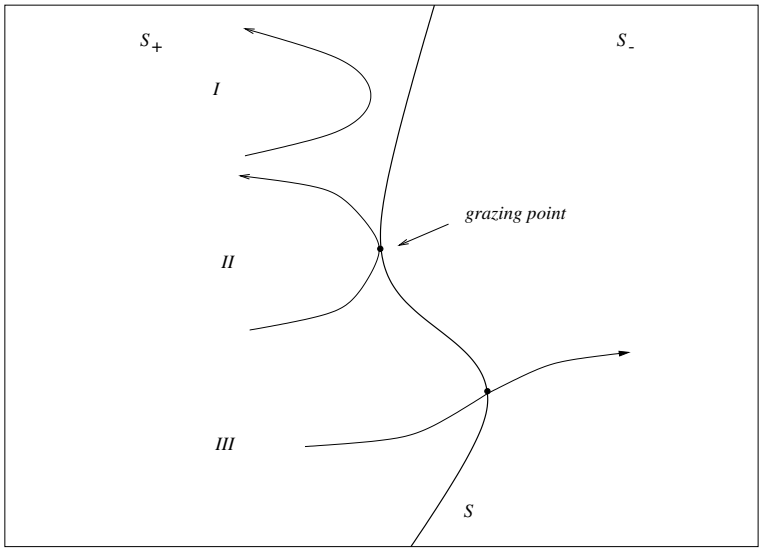

Figure 1: Schematic description of the system trajectory near a smooth phase-space boundary, Σ. The trajectory can evolve entirely in region S_1 without crossing the boundary (case I), hit it tangentially at a grazing point (case II) or cross the boundary and start evolving in region S_2 (case III).

1999, Banerjee & Grebogi 1999]). In particular, a qualitative change of the system behaviour is usually observed when a part of the system trajectory hits tangentially one of the boundaries between different regions in phase space. When this occurs the system is said to undergo a *grazing* bifurcation, also known as C-bifurcations in the Russian literature (see Fig. 1) [Nordmark 1991], Feigin [1970, 1974, 1978]. These events are often studied in the case of specific low-dimensional physical systems such as, for example, impact oscillators [Babitskii 1978, Shaw & Holmes 1983*a*, Foale & Bishop 1994, Whiston 1987] and power electronic converters [di Bernardo, Champneys & Budd 1998, di Bernardo, Garofalo, Glielmo & Vasca 1998].

Following the original approach presented in [Nordmark 1991], the analysis is usually carried out by finding an appropriate local map describing the system dynamics in a neighborhood of the grazing event [Chin, Ott, Nusse & Grebogi 1994, Foale & Bishop 1994, Foale 1994, Budd & Dux 1994*b*, di Bernardo et al. 1999]. This *normal form* is then used to classify the bifurcation scenarios following grazing. These can include several nonstandard transitions including the aforementioned "jump" from a periodic solution to a chaotic attractor.

In the case of two-dimensional impact oscillators, for instance, where a particle hits a rigid wall, the local map, also known as the Nordmark map, was found to contain a square root singularity [Nordmark 1991]. The dynamics of such a map was studied by Chin et al. [1994] and shown to give rise to a plethora of complex phenomena including the so-called "period-adding" cascade. Note that the impacting event in this system is modelled by means of a coefficient of restitution law which introduces a discontinuity in the system states at each impact [Thompson & Ghaffari 1983], which is equivalent to a δ-function-type discontinuity in the vector field F of equation (1.1). This analysis was recently generalized to n-dimensional impact oscillators in Frederiksson & Nordmark [2000].

Independent work reported in Nusse & Yorke [1995, 1992, 1994] and Feigin [1970, 1974, 1978, 1995, 1996] confirmed that these complex phenomena are qualitatively similar to those observed in discrete-time piecewise linear maps undergoing a so-called *border collision* bifurcation. This bifurcation occurs when a periodic point of the map crosses one of the boundaries. Moreover, as recently expounded in [di Bernardo et al. 1999], Feigin goes further and offers a first attempt to explain the relationship between grazing and border collision. In fact, he conjectures that the dynamics near grazing of a general n-dimensional PWS system can be described by piecewise-linear local maps. Thus, under an appropriate choice of coordinates, the grazing of a limit-cycle of the original PWS system corresponds to the border-collision of its normal form. This idea was independently used by Yuan, Banerjee, Ott & Yorke [1998] where the classification of the dynamics close to a grazing in a widely used electrical circuit is carried out successfully and confirmed by experiments.

Summarizing the above literature, one might conclude that the dynamics of a PWS system near grazing are described by:

- local maps with a square-root singularity if the vector field has an impulsive discontinuity across different regions in phase space (as in impact oscillators);
- piecewise linear normal forms if the states are continuous across the phase space boundaries but the vector field is not.

This gives rise to several interesting issues. For instance, in the case of oscillators with non-instantaneous impacts (such as would occur for example with a particle hitting a compliant but stiff wall) one should expect convergence towards a square-root singularity as the duration of the impacts is made shorter and shorter [Shaw & Holmes 1983*b*, Frederiksson & Nordmark 1997, Nordmark 1997]. At present, it is difficult to account for this transition analytically due to the lack of a consistent general theory for the derivation of appropriate local mappings in n-dimensional PWS systems near-grazing.

The first step of such a consistent theory have been presented in a recent paper by Dankowicz & Nordmark [1999]. Specifically, in the course of their study of a class of friction oscillators, they applied the concept of a *discontinuity mapping* to analyse the local dynamics near grazing of arbitrary autonomous vector fields which are continuous across the boundary. As set out in detail in Sec. 2.2 below, this mapping is defined as the "correction" that must be applied to the system trajectory in order to account for the presence of the switching or impacting boundary in phase space. This powerful concept allows the formal derivation of stroboscopic Poincaré mappings for general non-smooth dynamical systems undergoing grazings. For a particular class of vector field that is continuous across the discontinuity boundary, but with discontinuous Jacobian there, they show that the discontinuity mapping has a 3/2 power-law singularity. They then go on to examine the dynamical consequences of this for the friction oscillator example, showing that globally period-adding bifurcations and chaos may occur for such a mapping also.

The analysis of Dankowicz & Nordmark [1999] is based on the use of the Implicit Function Theorem but unfortunately does not allow easy and immediate comparison between local maps associated with different properties of the vector fields. Moreover, in its original formulation the discontinuity mapping takes zero time and is only really appropriate when studying Poincaré maps which are defined stroboscopically in time for T-periodic non-autonomous systems.

In this paper we present a general strategy for the derivation of appropriate local maps near grazing for n-dimensional PWS systems. Our analysis is based on the use of asymptotics and power series expansions which yield a synthetic analytical description of the grazing normal form for a generic PWS system. Our work extends the results presented in [Dankowicz & Nordmark 1999] in three ways:

- we do not assume the vector field is continuous across the boundary but allow for arbitrary jumps in either the vector field or its derivatives, with the only restriction being that the jumps must be such that there is no possibility of a so-called sliding solution (i.e. a solution evolving along the boundary itself);
- we introduce a preliminary stage where the discontinuity boundary is flattened locally through an *a priori* near-identity transformation which leads to much simpler final forms of the local maps and the possibility of writing general expressions for these maps;
- we define the new concept of a Poincaré-section discontinuity mapping which is more general than the zero-time mapping and enables the study of grazing periodic orbits in both autonomous and non-autonomous systems.

The result is a general formula for the normal form map that describes a grazing bifurcation in n-dimensional PWS systems. In particular, we present three alternative derivations of such local mappings which give both a heuristic and more rigorous description of the system dynamics near grazing. This allow the immediate comparison of systems characterized by both continuous and discontinuous vector fields across the boundary

and the derivation of their corresponding normal forms. In this sense, our work extends and encompass the ideas presented in [Dankowicz & Nordmark 1999].

Surprisingly, the main results of our investigation suggest that a **square-root singularity**, similar to the one contained in the Nordmark map, has to be expected only if the vector field is discontinuous at the grazing point. In all other cases, provided that either the first or second derivative of the vector field is discontinuous at the grazing point, a **singularity of order** $\frac{3}{2}$ is observed instead. Thus, we claim that **piecewise-linear** local maps are not seen generically for systems with smooth boundaries. In contrast, a piecewise-linear map can indeed be derived, as shown in [di Bernardo, Budd & Champneys 2000*b*], when the boundary itself has a corner-type singularity, and a trajectory undergoes a so-called *corner collision* grazing at the boundary. Incidentally, the system in [Yuan et al. 1998] falls precisely into this latter class because the phase space boundary is given by a sawtooth function and grazing occurs precisely at the corner of the sawtooth.

The rest of the paper is structured as follows. After stating our main assumptions, in Sec. 2 the concepts of grazing and discontinuity mappings are carefully introduced. Sec. 2 then goes on to state the main results of our investigation, the derivation is given in Secs. 3 and 4 where a local analysis of the dynamics near-grazing is carried out. This is based on three different stages according to whether the trajectory is on one side of the phase-space boundary or the other. Thus, we will study the motion before the first crossing of the boundary (Sec. 3.1), on the other side of the boundary (Sec. 3.2) and after its second crossing (see Sec. 3 and Fig. 4 for further details). As mentioned above, this third stage is developed in three alternative ways. First a heuristic description is presented in Sec. 3.3.1, then the zero-discontinuity mapping and the Poincaré discontinuity mapping are derived in Secs. 3.3.2 and 3.3.3 respectively. The application of these maps to the analysis of periodic orbits which graze is outlined in Sec. 4. Finally, Secs. 5 and 6 present numerical applications to a bilinear oscillator and to higher-order systems, which perfectly illustrate the theory.

2 Grazing in piecewise-smooth dynamical systems

2.1 Assumptions

We will focus our attention on n-dimensional piecewise-smooth sets of autonomous ODEs (1.1) which for small x we assume can be written in the form

$$\dot{x} = \begin{cases} F_1(x), & \text{if } H(x) > 0 \\ F_2(x), & \text{if } H(x) < 0 \end{cases}, \tag{2.1}$$

where $x \in \mathbb{R}^n$,$F_1, F_2 : \mathbb{R}^n \mapsto \mathbb{R}^n$ are supposed to be sufficiently smooth, $H : \mathbb{R}^n \mapsto \mathbb{R}$ is a sufficiently smooth (at least C^4) scalar function of the system states, which defines a phase space boundary between regions of smooth dynamics, and, for the time being, we have suppressed the parameter dependence in F. Note that non-autonomous dynamical systems can be put in the form (2.1) by considering time as an extra state variable described by the equation $\dot{t} = 1$ and making the phase space cyclic in the t-coordinate direction (e.g. a cylinder).

According to (2.1), H defines the set

$$S := \{x \in \mathbb{R}^n : H(x) = 0\}$$

which is termed the *switching manifold*. S divides the phase space locally into two regions

$$S^+ = \{x \in \mathbb{R}^n : H(x) > 0\}$$
$$S^- = \{x \in \mathbb{R}^n : H(x) < 0\}$$

associated with the two functional forms F_1 and F_2 respectively. We assume that both the vector fields F_1 and F_2 are defined over the entire local region of phase space under consideration, i.e., on both sides of S.

Thus, the flows Φ_i, $i = 1, 2$, generated by each of the vector fields can be defined as the quantities that satisfy

$$\frac{\partial}{\partial t}\Phi_i(x,t) = F_i(\Phi_i(x,t)), \qquad \Phi(x,0) = x\,. \tag{2.2}$$

Without loss of generality, we say that a *grazing* occurs at $x = 0$ if the following conditions are satisfied for $i = 1, 2$:

$$H(0) = 0, \tag{2.3}$$

$$\nabla H(0) \neq 0, \tag{2.4}$$

$$\langle \nabla H^0, \frac{\partial \Phi_i}{\partial t}(0,0)\rangle = \langle \nabla H^0, F_i^0\rangle = 0, \tag{2.5}$$

$$\left.\frac{d^2 H(\Phi(0,t))}{dt^2}\right|_{t=0} = \left\langle \nabla H^0, \frac{\partial F_i^0}{\partial x} F_i^0 \right\rangle + \left\langle \frac{\partial^2 H}{\partial x^2} F_i^0, F_i^0 \right\rangle > 0, \tag{2.6}$$

where a superscript '0' denotes quantities evaluated at $x = 0$. The first two conditions state that H is a good function for defining the switching manifold. The third condition states that grazing takes place at the origin of x, i.e. that the vector field there is tangent to S. The final condition ensures that the curvature of the trajectories in S^+ and S^- is of the same sign with respect to H and without loss of generality we assume this sign to be positive.

In addition, we will also assume that in a sufficiently small neighborhood of the grazing point, no Filippov solution (or sliding) can take place [Filippov 1988]. Such a solution can be seen heuristically as a motion taking place along the discontinuity surface in the limit of infinitely many switchings. A necessary condition to avoid sliding is that, under the flow of system (2.1) sufficiently close to the grazing point, the boundary $\{H = 0\}$ should never be simultaneously attracting (or repelling) from both sides S^+ and S^-; that is

$$\langle \nabla H, F_1\rangle\langle \nabla H, F_2\rangle > 0, \qquad 0 < \|x\| \leq \epsilon. \tag{2.7}$$

for some $\epsilon > 0$.

The trajectory, $x = x_g(t)$, generated by the flow $\Phi_i(0,t)$, which satisfies the grazing conditions listed above for $t = 0$, is termed the *grazing trajectory.* The *grazing sets*, L_{gi}, $i = 1, 2$, are defined as:

$$L_{gi} := \{x \in S | \langle \nabla H, F_i(x)\rangle = 0\}, \qquad i = 1, 2 \tag{2.8}$$

Note that, condition (2.7) implies that

$$L_{g1} \equiv L_{g2}. \tag{2.9}$$

i.e., L_{g1} and L_{g2} must coincide otherwise there will be regions where sliding is possible (see Fig. 2).

In the analysis that follows it will be helpful to assume that S is flat up to a sufficiently high order. That is $(\partial^i H^0)/(\partial x^i) \equiv 0$ for $i = 2, \ldots, N$ for some N. Note that this may be assumed without loss of generality by making a series of near-identity transformations of form

$$\tilde{x} = x + \frac{1}{2}\sum \frac{\partial^2 H^0}{\partial x_i \partial x_j} x_i x_j \frac{\nabla H^0}{\|\nabla H^0\|}, \qquad \tilde{H}(\tilde{x}) = H(x), \quad \tilde{F}(\tilde{x}) = F(x), \tag{2.10}$$

$$\tilde{\tilde{x}} = \tilde{x} + \frac{1}{6}\sum \frac{\partial^3 \tilde{H}^0}{\partial \tilde{x}_i \partial \tilde{x}_j \partial \tilde{x}_k} \tilde{x}_i \tilde{x}_j \tilde{x}_k \frac{\nabla H^0}{\|\nabla H^0\|}, \qquad \tilde{\tilde{H}}(\tilde{\tilde{x}}) = \tilde{H}(\tilde{x}), \quad \tilde{\tilde{F}}(\tilde{\tilde{x}}) = \tilde{F}(\tilde{x}), \tag{2.11}$$

etc.

It will transpire that removing the derivatives of H up to order four is sufficient for our purposes. Henceforth we shall assume that such sequence of transformations (2.10), (2.11) has been made, and we shall drop the tildes on the new variables.

In terms of the new variables the last two conditions (2.6) then be simplified to read

$$\left.\frac{d^2 H(\Phi(0,t))}{dt^2}\right|_{t=0} = \left\langle \nabla H^0, \frac{\partial F_i^0}{\partial x} F_i^0 \right\rangle > 0. \tag{2.12}$$

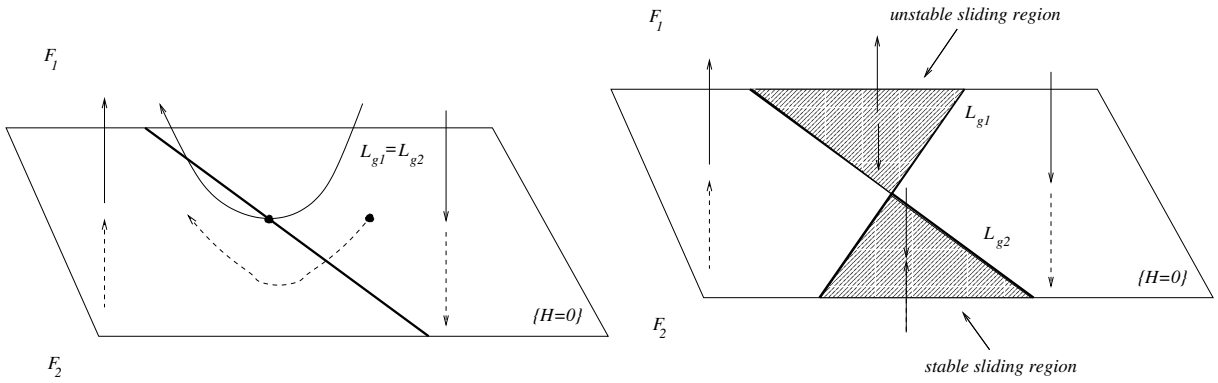

Figure 2: Grazing lines as defined by (2.8) in a representative three-dimensional example when they do (a) and do not (b) coincide. Note that if they do not coincide, the gradients of the system flows imply that there are two regions where sliding is possible (one stable and the other unstable).

Also, if we assume that (2.9) holds so that $L_{g1} = L_{g2} := L_g$, then (2.7) can be simplified to

$$\langle L, F_1^0 \rangle \langle L, F_2^0 \rangle > 0, \tag{2.13}$$

where L is a unit vector perpendicular to ∇H^0 and L_g^0. Condition (2.13) is arrived at by requiring that at the grazing point the grazing manifold L_g is not attractive. Note that it has the advantage over (2.7) in that it only involves quantities evaluated at the grazing point.

Because of the smoothness of the vector fields, we can expand the system flows $\Phi_i(x,t)$ as a Taylor series about the grazing point $(0,0)$ as:

$$\begin{aligned}
\Phi_i(x,t) &= \Phi_i^0 + \frac{\partial \Phi_i^0}{\partial x}x + \frac{\partial \Phi_i^0}{\partial t}t + \frac{1}{2}\frac{\partial^2 \Phi_i^0}{\partial x^2}x^2 + \frac{1}{2}\frac{\partial^2 \Phi_i^0}{\partial t^2}t^2 \frac{\partial^2 \Phi_i^0}{\partial x \partial t}xt \\
&+ \frac{1}{6}\left(\frac{\partial^3 \Phi^0}{\partial x^3}x^3 + \frac{\partial^3 \Phi^0}{\partial t^3}t^3 + 3\frac{\partial^3 \Phi^0}{\partial x \partial t^2}xt^2 + 3\frac{\partial^3 \Phi^0}{\partial x^2 \partial t}x^2 t\right) + \\
&+ \frac{1}{24}\left(\frac{\partial^4 \Phi_i^0}{\partial x^4}x^4 + \frac{\partial^4 \Phi_i^0}{\partial t^4}t^4 + 4\frac{\partial^4 \Phi_i^0}{\partial x^3 \partial t}x^3 t + 6\frac{\partial^4 \Phi_i^0}{\partial x^2 \partial t^2}x^2 t^2 + 4\frac{\partial^4 \Phi_i^0}{\partial x \partial t^3}xt^3\right) + \ldots
\end{aligned} \tag{2.14}$$

Note that we have used a shorthand notation here for the higher-order derivative terms, for example

$$\frac{\partial^3 \Phi^0}{\partial x^3}x^3 = \sum_{i,j,k=1,2,3} \frac{\partial^3 \Phi^0}{\partial x_i x_j x_k} x_i x_j x_k \, .$$

In what follows, we shall continue to use this shorthand, with care taken to correctly evaluate the derivative tensors when required. Also, for the sake of simplicity, we will omit the superscript 0. Thus, unless specified otherwise, all the quantities are evaluated at the grazing point $(x,t) = (0,0)$.

Using the second expression in (2.2) and the fact that

$$\frac{\partial^2 \Phi}{\partial t^2} = \frac{\partial F_i^0}{\partial t} = \frac{\partial F_i^0}{\partial \Phi_i}\frac{\partial \Phi_i^0}{\partial t} = \frac{\partial F_i^0}{\partial x}F_i^0,$$

we obtain from (2.14) that

$$\begin{aligned}
\Phi_i(x,t) &= x + F_i t + \frac{1}{2}\frac{\partial F_i}{\partial x}F_i t^2 + \frac{\partial F_i}{\partial x}xt \\
&+ \frac{1}{6}\left(\frac{\partial^2 F_i}{\partial x^2}F_i^2 + \left(\frac{\partial F_i}{\partial x}\right)^2 F_i\right)t^3 + \frac{1}{2}\frac{\partial^2 F_i}{\partial x^2}x^2 t + \frac{1}{2}\left(\frac{\partial^2 F_i}{\partial x^2}F_i + \left(\frac{\partial F_i}{\partial x}\right)^2\right)xt^2
\end{aligned}$$

$$
\begin{aligned}
&+ \quad \frac{1}{24}\left[\frac{\partial^3 F_i}{\partial x^3}F_i^3 + \frac{\partial^2 F_i}{\partial x^2}\left(F_i\frac{\partial F_i}{\partial x} + \frac{\partial F_i}{\partial x}F_i\right) + \left(\frac{\partial^2 F_i}{\partial x^2}\frac{\partial F_i}{\partial x} + \frac{\partial F_i}{\partial x}\frac{\partial^2 F_i}{\partial x^2}\right)F_i\right. \qquad (2.15)\\
&+ \quad \left.\left(\frac{\partial F_i}{\partial x}\right)^3 F_i\right]t^4 + \frac{1}{6}\frac{\partial^3 F_i}{\partial x^3}x^3 t + \frac{1}{4}\left(\frac{\partial^3 F_i}{\partial x^3}F_i + \frac{\partial F_1}{\partial x}\frac{\partial^2 F_i}{\partial x^2}\right)x^2 t^2 + \frac{1}{6}\left[\frac{\partial^3 F_i}{\partial x^3}F_i^2\right.\\
&+ \quad \left.\frac{\partial^2 F_i}{\partial x^2}\frac{\partial F_i}{\partial x}F_i + \frac{\partial^2 F_i}{\partial x^2}F_i\frac{\partial F_i}{\partial x} + \left(\frac{\partial^2 F_i}{\partial x^2}F_i\frac{\partial F_i}{\partial x} + \frac{\partial F_i}{\partial x}\frac{\partial^2 F_i}{\partial x^2}F_i\right) + \left(\frac{\partial F_i}{\partial x}\right)^3\right]xt^3\\
&:= \quad x + F_i t + a_i t^2 + b_i xt + c_i t^3 + d_i x^2 t + e_i xt^2 + f_i t^4 + g_i x^3 t + h_i x^2 t^2 + j_i xt^3 + O(5),
\end{aligned}
$$

where the remainder term $O(5)$ is a shorthand for terms involving monomials in (x,t) of order at least 5.

Notice that, linearizing system (2.1) in a sufficiently small neighborhood of the grazing point $(0,0)$, we obtain

$$
\dot{x} = \begin{cases} A_1 x + B_1, & \text{if } H(x) > 0 \\ A_2 x + B_2, & \text{if } H(x) < 0 \end{cases},
$$

where

$$
A_i = \frac{\partial F_i^0}{\partial x}, \qquad B_i = F_i^0.
$$

Thus, the vector field is continuous at the grazing point $(x = 0, t = 0)$ if $B_1 = B_2$, while the vector field is discontinuous if $B_1 \neq B_2$.

2.2 Discontinuity Mapping

As mentioned in the introduction, the main aim of this paper is that of presenting a comprehensive strategy for the derivation of appropriate local mappings in a neighborhood of the grazing event for n-dimensional piecewise-smooth dynamical systems. For this purpose, we briefly summaries here the concept of the so-called *discontinuity mapping* which was introduced in [Dankowicz & Nordmark 1999] and will be used later in Sec. 3.3.2.

The discontinuity map can be defined as the correction to be made to the system trajectories in order to account for the presence of a switching manifold in phase space. Its algebraic construction will be described later, in Sec. 3.3.2, but is depicted graphically in Fig. 3. Specifically, take a trajectory such as the one depicted in Fig. 3 and suppose that it intersects some Poincaré section Σ_1 at some time $t_s < 0$ and a second Poincaré section, Σ_2 at some time $t_f > 0$ (see Fig. 4). In order to compute such a trajectory from Σ_1 to Σ_2, we would compute the first segment (from Σ_1 to $\bar{x}$) using flow 1. Then, we would consider the second flow (from $\bar{x}$ to $\hat{x}$) to take into account the fact that the system has crossed the switching manifold. Finally, we would use again flow 1 to compute the third segment of the trajectory (from $\hat{x}$ to Σ_2).

Alternatively, we could use flow 1 to compute the trajectory until it reaches a given reference section (e.g. the plane Π in Fig. 3), even if it crosses the switching manifold. At this point, we would apply the discontinuity mapping to take into account the fact that the manifold has been crossed. Finally, we would apply again flow 1 to compute the final part of the trajectory from the corrected initial point on Π to the desired Poincaré section Σ_2.

We term this mapping the *Poincaré discontinuity mapping* (PDM). This is a generalization of the mapping introduced in [Dankowicz & Nordmark 1999] which we term the *zero-time discontinuity mapping* (ZDM), that is the map obtained by considering the zero-time correction needed to take into account the presence of the boundary. The ZDM will be particularly useful for describing the local dynamics of non-autonomous systems while the PDM will be more suitable to construct global maps for periodic orbits which graze (for more details see Sec. 3.3.2 and 3.3.3 below).

In this sense, the discontinuity mapping represents the correction brought about by the presence of the switching manifold. It is obvious, as will be shown later, that the construction of both the PDM and ZDM requires knowledge of both the flows on each side of the switching manifold.

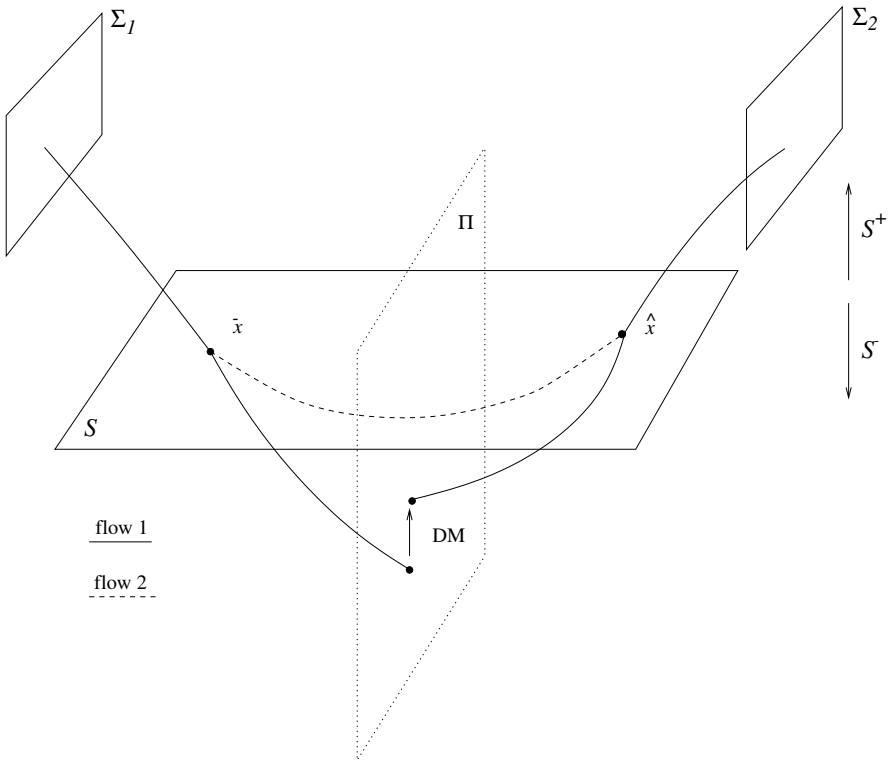

Figure 3: A graphical explanation of the Discontinuity Mapping (DM)

2.3 The results

Using these mappings, the local dynamics of the system near grazing can be effectively described analytically. In the rest of the paper we shall show that there is a fundamental difference between systems that are continuous at the grazing point, and ones that are discontinuous. Specifically, Section 3 below is devoted to a proof of the following theorem.

Theorem 1 *Given the assumptions (2.3)–(2.6), (2.9), (2.12) and (2.13), then, as defined in Sec. 3, the local discontinuity mappings (DM) describing trajectories in a neighbourhood of the grazing trajectory have: a 3/2-type singularity at the grazing point in the case where* $F_1^0 = F_2^0$ *while* $\frac{\partial F_1}{\partial x} \neq \frac{\partial F_2}{\partial x}$ *or* $\frac{\partial^2 F_1}{\partial x^2} \neq \frac{\partial^2 F_2}{\partial x^2}$*; and a square-root singularity if* $F_1^0 \neq F_2^0$.

Note in particular that we never see the case of a piecewise-linear discontinuity mapping.

Section 4 then goes on to consider the neighbourhood of a periodic orbit that grazes. The results there can be summarized in the following theorem which for simplicity we state here for a time-T stroboscopic map for an mT-periodic orbit in a T-periodic non-autonomous system. Similar, but slightly more complicated expressions hold for the more general case of a Poincaré map around a periodic orbit in an autonomous system (see formulae (4.4) and (4.5) below).

Theorem 2 *If the grazing trajectory is part of a hyperbolic* mT*-periodic orbit* $p(t)$ *that grazes at a parameter value* $\mu = 0$*, then the Poincaré map defined in a neighbourhood of* $p(t)$ *can be written locally as follows.*

1. *If the vector field is discontinuous at grazing we have:*

$$x \mapsto \begin{cases} Nx + M\mu, & \text{if } \langle \nabla H, x \rangle > 0 \\ N\mathbf{w}\sqrt{|\langle \nabla H, x \rangle|} + M\mu + h.o.t. & \text{if } \langle \nabla H, x \rangle < 0, \end{cases}$$

where

$$\mathbf{w} = 2(F_2 - F_1)\frac{\langle \nabla H, \frac{\partial F_2}{\partial x} F_1 \rangle}{\langle \nabla H, \frac{\partial F_2}{\partial x} F_2 \rangle} \left(\frac{2}{\langle \nabla H, \frac{\partial F_1}{\partial x} F_1} \right)^{\frac{1}{2}},$$

and N, M are appropriate matrices and vectors describing the linearized Poincaré map for non-border-crossing trajectories in a neighbourhood of $p(t)$ (see Sec. 4 below for precise definition).

2. *If the vector field is continuous, i.e. $F_1 = F_2 := F$, but has discontinuous first derivative:*

$$x \mapsto \begin{cases} Nx + M\mu, & \text{if } \langle \nabla H, x\rangle > 0 \\ N\left(x + \mathbf{v}_1(|\langle \nabla H, x\rangle|)^{\frac{3}{2}} + V_2 x(|\langle \nabla H, x\rangle|)^{\frac{1}{2}} + \mathbf{v}_3\langle \nabla H, \frac{\partial F_2}{\partial x}x\rangle(|\langle \nabla H, x\rangle|)^{\frac{1}{2}}\right) + M\mu + h.o.t & \text{if } \langle \nabla H, x\rangle < 0 \end{cases}$$

where

$$\begin{aligned}
\mathbf{v}_1 &= \frac{1}{\langle \nabla H, \frac{\partial F_1}{\partial x}F_1\rangle^{\frac{3}{2}}}\left\{\frac{2}{3}\left(\frac{\partial^2 F_2}{\partial x^2} - \frac{\partial^2 F_1}{\partial x^2}\right)F^2 + 2\frac{\partial F_2}{\partial x}\frac{\partial F_1}{\partial x}F - \frac{2}{3}\left[\left(\frac{\partial F_1}{\partial x}\right)^2 + 2\left(\frac{\partial F_2}{\partial x}\right)^2\right]F\right. \\
&\quad - \frac{2}{\langle \nabla H, \frac{\partial F_2}{\partial x}F_2\rangle}\left(\frac{\partial F_2}{\partial x} - \frac{\partial F_1}{\partial x}\right)F\left[\frac{2}{3}\left\langle \nabla H, \left(\frac{\partial^2 F_2}{\partial x^2}F_2^2 + \left(\frac{\partial F_2}{\partial x}\right)^2 F_2\right)\right\rangle\right. \\
&\quad \left.\left. + \left\langle \nabla H, \left(\frac{\partial F_2}{\partial x}\frac{\partial F_1}{\partial x} - 2\left(\frac{\partial F_2}{\partial x}\right)^2\right)F\right\rangle + \langle \nabla H, \frac{\partial^2 F_2}{\partial x}F^2, \rangle\right]\right\} \\
V_2 &= \frac{2}{\sqrt{\langle \nabla H, \frac{\partial F_1}{\partial x}F_1\rangle}}\left(\frac{\partial F_2}{\partial x} - \frac{\partial F_1}{\partial x}\right) \\
\mathbf{v}_3 &= \frac{2}{\langle \nabla H, \frac{\partial F_2}{\partial x}F_2\rangle\sqrt{\langle \nabla H, \frac{\partial F_1}{\partial x}F_1\rangle}}\left(\frac{\partial F_2}{\partial x}F_2 - \frac{\partial F_1}{\partial x}F_1\right).
\end{aligned}$$

3 Local Analysis

Throughout this section we shall consider only points (x,t) sufficiently close to the grazing point $(0,0)$, specifically those points lying in a ball of radius ϵ, $\|x\| < \epsilon$, $|t| < \epsilon$, for some sufficiently small $\epsilon > 0$. Assume that system (2.1) has a grazing orbit lying entirely in region S^+ in a neighborhood of the grazing point $x = 0$, i.e., an orbit verifying conditions (2.3)–(2.6), (2.9), (2.12) and (2.13). Moreover, suppose that this orbit intersects some Poincaré section Σ_1 at time $t_s < 0$ and a second Poincaré section, Σ_2 at some time $t_f > 0$ (see Fig. 4). Introduce a coordinate ε on Σ_1 such that when $\varepsilon = 0$ the orbit grazes the switching manifold S, while for $\varepsilon \neq 0$ it either crosses the boundary for $\varepsilon > 0$ or remains in S^+ if $\varepsilon < 0$.

We now seek to investigate the local dynamics of system (2.1) in a neighborhood of the grazing point by varying ε and observing the corresponding changes of the Poincaré intersections on Σ_2. In so doing, we will divide the analysis into three different stages:

1. Motion in S^+ before the first crossing of the switching manifold at $t = t_1 < 0, x = \bar{x}$;
2. Motion in S^- until the crossing of S at $t = t_2 > 0, x = \hat{x}$;
3. Motion in S^+ after the second crossing of S.

In fact, the PDM as defined in the previous section is in effect defined by taking the limit as both Σ_1 and Σ_2 tend to Π, but it may be helpful conceptually to consider motion between two hypothetical surfaces Σ_1 and Σ_2 as drawn.

3.1 Step 1: Motion before the first crossing of S

Let $x_g(t) = \Phi_1(0,t)$ be the grazing trajectory existing for $\varepsilon = 0$, and consider perturbations of x_g of size ε such that:

$$x(t) = \Phi_1(\varepsilon x_0, t)$$

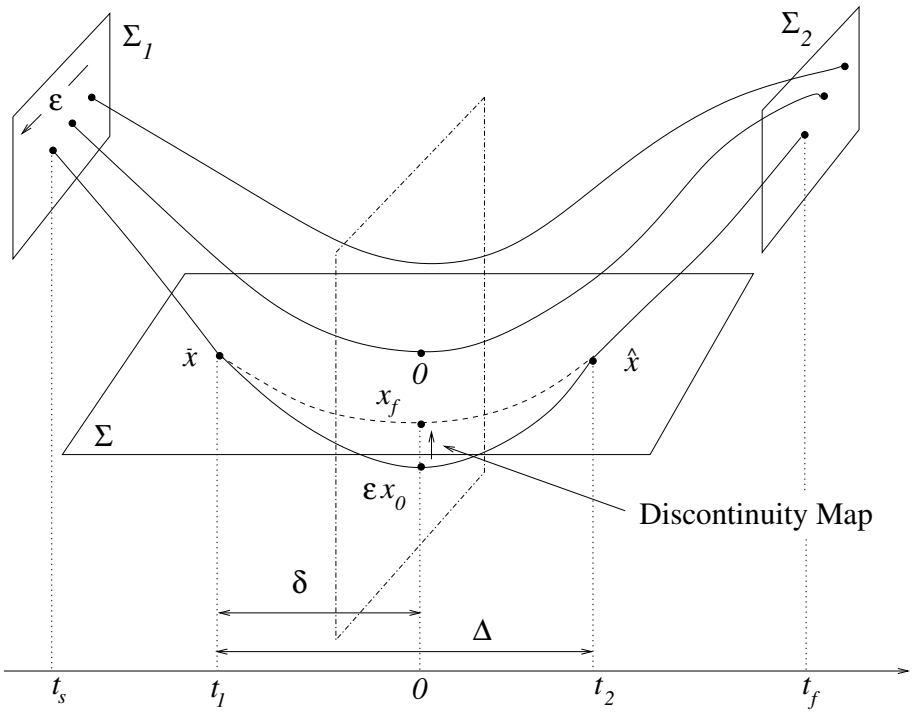

Figure 4: Local analysis of grazing. A sketch graph of the three-dimensional case

for some x_0 which we assume to be such that:

$$\langle \nabla H, x_0 \rangle < 0. \tag{3.1}$$

This ensures that for $\varepsilon > 0$ we are analyzing a trajectory that really does cross $\{H = 0\}$, even if we consider it as being entirely generated by the first flow with initial condition εx_0. Specifically, if $\varepsilon > 0$, then at some time $t_1 = -\delta$ the perturbed trajectory, $x(t)$, will cross the switching manifold at $x = \bar{x}$ given by

$$\begin{aligned} \bar{x} &= \Phi_1(\varepsilon x_0, -\delta) = \varepsilon x_0 - \delta F_1 + \delta^2 a_1 - \varepsilon\delta b_1 x_0 - \delta^3 c_1 - \varepsilon^2 \delta d_1 x_0^2 + \varepsilon\delta^2 e_1 x_0 \\ &\quad + \delta^4 f_i - \varepsilon^3 \delta g_1 x_0^3 + \varepsilon^2\delta^2 h_1 x_0^2 - \varepsilon\delta^3 j_1 x_0 + O(5), \end{aligned} \tag{3.2}$$

where we have used the Taylor expansion (2.15) up to fourth-order terms.

We wish to define δ to be the time such that $H(\bar{x}) = 0$, which since $H(0) = 0$ and H is flat up to order 4, implies

$$\langle \nabla H, \bar{x} \rangle = O(\|\bar{x}\|^5). \tag{3.3}$$

Using the expansion (3.2) for $\bar{x}$, (3.3) becomes

$$\begin{aligned} &\varepsilon x_{0H} - \delta F_{1H} + \delta^2 a_{1H} - \varepsilon\delta (b_1 x_0)_H - \delta^3 c_{1H} - \varepsilon^2 \delta (d_1 x_0^2)_H + \varepsilon\delta^2 (e_1 x_0)_H \\ &\quad + \delta^4 f_{1H} - \varepsilon^3 \delta (g_1 x_0^3)_H + \varepsilon^2\delta^2 (h_1 x_0^2)_H - \varepsilon\delta^3 (j_1 x_0)_H + O(5) = 0, \end{aligned} \tag{3.4}$$

where the subscript H denotes the component of a vector quantity along ∇H i.e.

$$y_H := \langle \nabla H, y \rangle.$$

Now the second term of (3.4) is $-\delta\langle \nabla H, F_1 \rangle$ which is zero by the grazing condition (2.5). Hence we can solve (3.4) for δ as an asymptotic expansion in $\sqrt{\varepsilon}$ with lowest order term $O(\varepsilon^{\frac{1}{2}})$. Note that there are two solutions but we are interested in the solution where δ is positive, and hence

$$\delta = \gamma_1 \varepsilon^{\frac{1}{2}} + \gamma_2 \varepsilon + \gamma_3 \varepsilon^{\frac{3}{2}} + O(\varepsilon^2) \qquad \text{where} \quad \gamma_1 = \sqrt{-\frac{x_{0H}}{a_{1H}}} = \sqrt{-2\frac{\langle \nabla H, x_0 \rangle}{\langle \nabla H, \frac{\partial F_1}{\partial x} F_1 \rangle}}. \tag{3.5}$$

Note by assumptions (2.12) and (3.1) that the quantity inside the square root is positive, hence by choosing ε small enough this is indeed a valid asymptotic expansion. Furthermore we obtain

$$\gamma_2 = \frac{(b_1 x_0)_H + c_{1H}\gamma_1^2}{2a_{1H}}, \tag{3.6}$$

$$\gamma_3 = -\frac{1}{2}\frac{a_{1H}\gamma_2^2 + (e_1 x_0)_H\gamma_1^2 - (b_1 x_0)_H\gamma_2 - 3c_{1H}\gamma_1^2\gamma_2 + f_{1H}\gamma_1^4}{a_{1H}\gamma_1}. \tag{3.7}$$

Hence, we can conclude that the time δ at which the perturbed trajectory, $x(t)$ crosses the switching manifold varies to lowest order as $\sqrt{\varepsilon}$. This will be shown to be extremely important in determining the overall local behaviour exhibited by the system when perturbations around the grazing point are considered.

3.2 Step 2: Motion in S^-

We now consider the piece of the perturbed orbit that lies in S^-. Then, starting from $x = \bar{x}$, we have that after some time $t_2 = \Delta$:

$$H(\hat{x}) := \Phi_2(\bar{x}, \Delta) = 0 \tag{3.8}$$

where $\bar{x}$ is given by the substitution of the expression (3.5) for δ into (3.2). That is,

$$\bar{x} = \chi_1\varepsilon^{\frac{1}{2}} + \chi_2\varepsilon + \chi_3\varepsilon^{\frac{3}{2}} + O(\varepsilon^2), \qquad \text{where} \quad \chi_1 = -F_1\gamma_1 \tag{3.9}$$

$$\text{and} \quad \chi_2 = x_0 - \gamma_2 F_1 + a_1\gamma_1^2, \tag{3.10}$$

$$\chi_3 = -b_1 x_0\gamma_1 + 2a_1\gamma_1\gamma_2 - \gamma_3 F_1 - c_1\gamma_1^3. \tag{3.11}$$

To get an approximation for Δ, we need to solve (3.8). As with the calculation of δ, we can simplify this condition to read

$$\langle \nabla H, \Phi_2(\bar{x}, \Delta)\rangle = O(\|\bar{x}\|^5),$$

which can be expanded as a Taylor series about the grazing point by using the expansion (2.15) for Φ_2 up to fourth-order terms. Thus we obtain

$$\begin{aligned}&\bar{x}_H + F_{2H}\Delta + a_{2H}\Delta^2 + (b_2\bar{x})_H\Delta + c_{2H}\Delta^3 + (d_2\bar{x}^2)_H\Delta + (e_2\bar{x})_H\Delta^2 \\ &\quad + \quad f_{2H}\Delta^4 + (g_2\bar{x}^3)_H\Delta + (h_2\bar{x}^2)_H\Delta^2 + (j_2\bar{x})_H\Delta^3 = O(5).\end{aligned} \tag{3.12}$$

Now $F_{2H} = \langle \nabla H, F_2\rangle = 0$ by the definition of grazing, and $\bar{x}_H = O(5)$ since $\bar{x} \in S$. Hence the first two terms of (3.12) can be removed and, after substitution of the expansion (3.9) for $\bar{x}$, the resulting expression can be solved for Δ as an asymptotic expansion in ε, ignoring the trivial solution $\Delta = 0$. Thus we obtain

$$\Delta = \nu_1\varepsilon^{\frac{1}{2}} + \nu_2\varepsilon + \nu_3\varepsilon^{\frac{3}{2}} + O(\varepsilon^2), \qquad \text{where} \quad \nu_1 = -\frac{(b_2\chi_1)_H}{a_{2H}} = \frac{\langle \nabla H, b_2 F_1\rangle\gamma_1}{\langle \nabla H, a_2\rangle}, \tag{3.13}$$

$$\text{and} \quad \nu_2 = -\frac{\nu 1\left[(d_2\chi_1^2)_H + c_{2H}\nu_1^2 + (b_2\chi_2)_H + (e_2\chi_1)_H\nu_1\right]}{2a_{2H}\nu_1 + (b_2\chi_1)_H}, \tag{3.14}$$

$$\begin{aligned}\nu_3 = &-\frac{(j_2\chi_1)_H\nu_1^3 + (b_2\chi_3)_H\nu_1 + a_{2H}\nu_2^2 + (2d_2\chi_1\chi_2)_H\nu_1 + (b_2\chi_2)_H\nu_2 + f_{2H}\nu_1^4}{2a_{2H}\nu_1 + (b_2\chi_1)_H} + \\ &-\frac{2(e_2\chi_1)_H\nu_1\nu_2 + 3c_{2H}\nu_1^2\nu_2 + (e_2\chi_2)_H\nu_1^2 + (h_2\chi_1)_H\nu_1^2 + (d_2\chi_1^2)_H\nu_2 + (g_2\chi_1^3)_H\nu_1}{2a_{2H}\nu_1 + (b_2\chi_1)_H}.\end{aligned} \tag{3.15}$$

Equation (3.13) is an estimate of the time Δ spent on the other side of the switching manifold in terms of the size of the initial perturbation ε. Note that the leading order term ν_1 is again $O(\varepsilon^{\frac{1}{2}})$ and is non-zero and finite by conditions (2.12) and (2.13). Hence the asymptotic expansion is valid.

3.3 Step 3: Motion after the second crossing of S

We look finally at the motion of the system after the second switching (i.e. when the trajectory crosses again the switching manifold). We shall present three alternative ways of carrying out the analysis. The first is heuristic and motivates the statement of Theorem 1 by showing how certain terms cancel in a Taylor expansion when simply comparing the trajectory in question with one that is governed by the flow Φ_1 alone. It turns out that this gives the right order of scaling for the local discontinuity mapping (DM) described in Sec. 2.2.

We then proceed to derive rigourously such a mapping in two separate ways. First, we calculate the DM taking zero time (the ZDM) and second the one calculated with respect to a Poincaré section (the PDM).

3.3.1 A heuristic calculation

We have that at $t = t_2 = \Delta - \delta$ the perturbed trajectory crosses the switching manifold again at $\hat{x}$ and enters the region S^+. Therefore, it can be compared directly with the unperturbed trajectory x_u obtained by considering the trajectory still rooted at $\bar{x}$ but generated by the first flow, i.e. $x_u(t) = \Phi_1(\bar{x}, t)$. Thus, at time $t = t_2$ we have:

$$\xi_0 := x(t_2) - x_u(t_2) = \Phi_2(\bar{x}, \Delta) - \Phi_1(\bar{x}, \Delta)$$

and expanding Φ_1 and Φ_2 about the grazing point, according to (2.14), we then get:

$$\begin{aligned}
\xi_0 &= (F_2 - F_1)\Delta + \frac{1}{2}\left(\frac{\partial F_2}{\partial x}F_2 - \frac{\partial F_1}{\partial x}F_1\right)\Delta^2 + \left(\frac{\partial F_2}{\partial x} - \frac{\partial F_1}{\partial x}\right)\bar{x}\Delta \\
&+ \frac{1}{6}\left[\left(\frac{\partial^2 F_2}{\partial x^2}F_2^2 + 2\left(\frac{\partial F_2}{\partial x}\right)^2 F_2\right) - \left(\frac{\partial^2 F_1}{\partial x^2}F_1^2 + 2\left(\frac{\partial F_1}{\partial x}\right)^2 F_1\right)\right]\Delta^3 \\
&+ \frac{1}{2}\left[\frac{\partial^2 F_2}{\partial x^2} - \frac{\partial^2 F_1}{\partial x^2}\right]\bar{x}^2\Delta \\
&+ \frac{1}{2}\left[\left(\frac{\partial^2 F_2}{\partial x^2}F_2 + \left(\frac{\partial F_2}{\partial x}\right)^2\right) - \left(\frac{\partial^2 F_1}{\partial x^2}F_1 + \left(\frac{\partial F_1}{\partial x}\right)^2\right)\right]\bar{x}\Delta^2 + \ldots
\end{aligned} \tag{3.16}$$

Now, as mentioned in Sec. 2.2, the discontinuity mapping (DM), as defined by Dankowicz and Nordmark [Dankowicz & Nordmark 1999], can be considered as the correction that must be added to a trajectory governed by flow Φ_1 alone in order to account for the time it spends in region S_-. Note there is some freedom as to the point on the trajectory to which this transformation is applied. Thus, we can see the vector ξ_0 defined by (3.16) as an approximation of such a correction at time t_2. In order to apply the DM at some other time instance we would simply have to evolve both the trajectories through $x(t_2)$ and $x_u(t_2)$ by flow Φ_1 through the *same* time-interval. Moreover since everything is local, by choosing ε small enough, this time of evolution will be sufficiently small to justify taking a linear approximation to Φ_1. Hence one ends up with simply a linear transformation of ξ_0, which does not affect the order of the leading-order singularity of the DM. Thus, we shall therefore view (3.16) as giving a heuristic form of the DM.

Now let us calculate the leading order term of ξ_0 as a function of ε. Since $\bar{x}$ and $\delta \sim \varepsilon^{1/2}$ by (3.5) and (3.9) then equation (3.16) shows that we can get $\varepsilon^{1/2}$, ε or $\varepsilon^{3/2}$ leading-order behaviour, depending on which is the first non-zero term in the expansion of ξ_0. Let us see which occurs under the assumption that the vector either is or is not continuous at the gazing point.

First, consider the case of discontinuity of the vector field at the grazing point,

$$F_2 \neq F_1.$$

Then the dominating term in (3.16) will be $(F_2 - F_1)\Delta$. Hence, from (3.13), we derive a $\sqrt{\varepsilon}$ local behaviour. That is

$$\xi_0 = (F_2 - F_1)\nu_1\varepsilon^{\frac{1}{2}} + O(\varepsilon) = 2(F_2 - F_1)\frac{\langle \nabla H, b_2 F_1\rangle}{\langle \nabla H, a_1\rangle}\sqrt{-2\frac{\langle \nabla H, x_0\rangle}{\langle \nabla H, a_1\rangle}}\,\varepsilon^{\frac{1}{2}} + O(\varepsilon), \tag{3.17}$$

the $O(\varepsilon^{\frac{1}{2}})$ term of which is generically non-zero.

If, instead, we assume that the vector field is continuous at the grazing point, then $F_1 = F_2$ at $x = 0$. Thus, in this case, the linear term in (3.16) disappears and the dominating term would appear to be the quadratic term:

$$\Theta := \frac{1}{2}\left(\frac{\partial F_2}{\partial x}F_2 - \frac{\partial F_1}{\partial x}F_1\right)\Delta^2 + \left(\frac{\partial F_2}{\partial x} - \frac{\partial F_1}{\partial x}\right)\bar{x}\Delta. \tag{3.18}$$

However, careful evaluation shows that this term is zero to leading order. Specifically, substitution of (3.9) and (3.13) into (3.18) yields

$$\Theta = \left[\frac{1}{2}\left(\frac{\partial F_2}{\partial x}F_2 - \frac{\partial F_1}{\partial x}F_1\right)\nu_1^2 + \left(\frac{\partial F_1}{\partial x}F_1 - \frac{\partial F_2}{\partial x}F_1\right)\nu_1\gamma_1\right]\varepsilon + O(\varepsilon^{\frac{3}{2}}) \tag{3.19}$$

and since $F_1 = F_2 := F$, we also have

$$\frac{\partial F_2}{\partial x}F_2 = \frac{\partial F_2}{\partial x}F_1 = \frac{\partial F_2}{\partial x}F$$

and from (3.13)

$$\nu_1 = 2\frac{\langle \nabla H, \frac{\partial F_2}{\partial x}F\rangle}{\langle \nabla H, \frac{\partial F_2}{\partial x}F\rangle}\gamma_1 = 2\gamma_1.$$

Thus, from (3.19), we get

$$\Theta = \left[2\left(\frac{\partial F_2}{\partial x} - \frac{\partial F_1}{\partial x}\right)F - 2\left(\frac{\partial F_2}{\partial x} - \frac{\partial F_1}{\partial x}\right)F\right]\gamma_1^2\varepsilon + O(\varepsilon^{\frac{3}{2}}) = 0 + O(\varepsilon^{\frac{3}{2}}).$$

Hence, if the vector field is continuous at the grazing point (but not necessarily anywhere else across the switching manifold), both the linear and quadratic terms in (3.16) disappear and since δ and $\bar{x} \sim \varepsilon^{1/2}$, ξ will vary as $\varepsilon^{3/2}$.

3.3.2 The zero-time discontinuity mapping (ZDM)

In order to define the ZDM we want to solve from the point $\hat{x} = \Phi_2(\bar{x}, \Delta)$, backwards in time using the flow Φ_1 through a time $-t_2 = \delta - \Delta$. The ZDM is then the map from the initial point εx_0 to this final point

$$x_f = \Phi_1(\hat{x}, \delta - \Delta).$$

Now using the Taylor expansion (2.15) for Φ_1 up to third-order terms we have

$$x_f = \hat{x} + F_1(\delta - \Delta) + a_1(\delta - \Delta)^2 + b_1\hat{x}(\delta - \Delta) + c_1(\delta - \Delta)^3 + d_1\hat{x}^2(\delta - \Delta) + e_1\hat{x}(\delta - \Delta^2) + O(4), \tag{3.20}$$

where

$$\hat{x} = \bar{x} + F_2\Delta + a_2\Delta^2 + b_2\bar{x}\Delta + c_2\Delta^3 + d_2\bar{x}^2\Delta + e_2\bar{x}\Delta^2 + O(4). \tag{3.21}$$

Thus, using the asymptotic expansions (3.5), (3.9), (3.13) and (3.21) for δ, $\bar{x}$, Δ and $\hat{x}$, we can systematically express x_f as a Taylor series in $\sqrt{\varepsilon}$. In order to prove Theorem 1, it suffices to consider in detail only the $O(\varepsilon^{\frac{1}{2}})$ and $O(\varepsilon)$ terms. For the case of continuity of the vector field at the grazing point (but discontinuity of its Jacobian or Hessian derivative there) we shall additionally need to show that the $O(\varepsilon^{\frac{3}{2}})$ term is non-zero. So let us first concentrate on the terms in x_f up to $O(\varepsilon)$. From (3.20), we obtain:

$$\begin{aligned} x_f = {} & \bar{x} + (F_2 - F_1)\Delta + F_1\delta \\ & + a_2\Delta^2 + b_2\bar{x}\Delta + a_1(\delta - \Delta)^2 + b_1(\delta - \Delta)(\bar{x} + F_2\Delta) + O(\varepsilon^{\frac{3}{2}}) \end{aligned} \tag{3.22}$$

Considering the case of discontinuity of the vector field at the grazing point $F_1 \neq F_2$, then the leading-order term in x_f is $O(\varepsilon^{\frac{1}{2}})$. Specifically

$$\begin{aligned} x_f &= \chi_1 \varepsilon^{\frac{1}{2}} + (F_2 - F_1)\nu_1 \varepsilon^{\frac{1}{2}} + F_1 \gamma_1 \varepsilon^{\frac{1}{2}} + O(\varepsilon) \\ &= -F_1\gamma_1\varepsilon^{\frac{1}{2}} + (F_2 - F_1)\nu_1\varepsilon^{\frac{1}{2}} + F_1\gamma_1\varepsilon^{\frac{1}{2}} + O(\varepsilon) = (F_2 - F_1)\nu_1\varepsilon^{\frac{1}{2}} + O(\varepsilon), \end{aligned} \tag{3.23}$$

which is the same as the leading order term (3.17) of ξ_0 for this case and is $O(\varepsilon^{\frac{1}{2}})$. This proves Theorem 1 for the case of a discontinuous vector field.

If, on the contrary we assume that the vector field is continuous at the grazing point, i.e. $F_1 = F_2$ then the $O(\varepsilon^{\frac{1}{2}})$ term in (3.23) obviously vanishes and the leading-order term would appear to be $O(\varepsilon)$. However, for apparently similar reasons to the cancelation that occured in the previous heuristic calculation, we will now show that this term is in fact equal to εx_0. Hence the ZDM is the identity up to this order, and the leading order non-trivial term is $O(\varepsilon^{\frac{3}{2}})$. Specifically, from (3.22), the $O(\varepsilon)$ term is

$$\Psi := \left(F_1\gamma_2 + \chi_2 + a_2\nu_1^2 + -b_2F_1\gamma_1\nu_1 + a_1(\gamma_1 - \nu_1)^2 + b_1(\gamma_1 - \nu_1)(F_2\nu_1 - F_1\gamma_1)\right)\varepsilon, \tag{3.24}$$

for which by the definition of χ_2, the first two terms are equal to $x_0 + a_1\gamma_1^2$.

Now, by similar arguments to those shown in Subsection 3.3.1 above, continuity at the grazing point implies

$$F_1 = F_2 := F, \quad \text{and hence} \quad \nu_1 = 2\gamma_1 \quad \text{and} \quad b_iF_j = b_iF_i = 2a_i, \tag{3.25}$$

with the latter equality being true because of the definition of a_i and b_i in (2.15). Hence (3.24) yields

$$\Psi = (x_0 + a_1\gamma_1^2 + 4a_2\gamma_1^2 - 4a_2\gamma_1^2 + a_1\gamma_1^2 - 2a_1\gamma^2)\varepsilon = \varepsilon x_0.$$

Hence the ZDM is the identity map up to $O(\varepsilon)$ and the leading-order non-trivial term is at least $O(\varepsilon^{\frac{3}{2}})$.

The expression for the $O(\varepsilon^{\frac{3}{2}})$ term can be written down in a systematic manner from (3.20) using (3.21), (3.5)–(3.7), (3.9)–(3.11), and (3.13)–(3.15). The algebraic manipulation package Maple was used to simplify the resulting expression using the relations (3.25). The result is

$$\begin{aligned} \Xi_{ZDM} := \; & \left[\left(8c_2 - c_1 + (e_1 - 4e_2)F + (2d_2 - d_1)F^2\right)\gamma_1^3 + \right. \\ & \left. + \left((2b_2 - b_1)\chi_2 + 2(a_2 - a_1)\nu_2\right)\gamma_1 + F_1\gamma_3 + \chi_3\right]\varepsilon^{\frac{3}{2}}, \end{aligned} \tag{3.26}$$

which is expressed purely in terms of F_1, F_2 and their derivatives in Appendix 1. Note from there that, unless a remarkable (non-generic) sequence of cancelations occurs, this term will be non-zero provided $\frac{\partial F_1}{\partial x} \neq \frac{\partial F_2}{\partial x}$. In fact, the formulae in the appendix also clearly reveal that the term is also non-zero if $\frac{\partial F_1}{\partial x} = \frac{\partial F_2}{\partial x}$ but $\frac{\partial^2 F_1}{\partial x^2} \neq \frac{\partial^2 F_2}{\partial x^2}$, that is if the vector field is C^1 across the boundary but not C^2. This then proves Theorem 1 for discontinuous vector fields.

3.3.3 The Poincaré section discontinuity mapping (PDM)

As motivated in Sec. 2.2, when coupling the dynamics of a DM to a global Poincaré map around a periodic orbit that grazes it is more useful not to compute a local DM that takes zero time, but to compute one which maps a certain Poincaré section back to itself. Note that in the case of a non-autonomous periodically forced system, the ZDM in effect calculates the PDM for the Poincaré section t=const. Hence by extending the phase space with a trivial equation $\dot{t} = 1$ if necessary, the PDM is a more general concept since it can be used to describe the adjustment to Poincaré maps around periodic orbits for both autonomous and periodically forced systems.

So let us suppose that the initial point εx_0 is on a Poincaré section Π which is defined by a normal vector $\boldsymbol{\pi}$. That is

$$\varepsilon x_0 \in \Pi, \quad \Pi := \{x : \langle \boldsymbol{\pi}, x \rangle = 0\}$$

where, to ensure that the flow is transverse to Π we require

$$\langle \boldsymbol{\pi}, F_i \rangle \neq 0, \qquad i = 1, 2\,. \tag{3.27}$$

We shall denote by a subscript π the projection along $\boldsymbol{\pi}$, that is

$$y_\pi = \langle \boldsymbol{\pi}, y \rangle.$$

Then in order to define x_f, instead of demanding that the transformation from εx_0 should take zero time, we shall demand that x_f is on the Poincaré section Π. That is $x_f = \Phi_1(\hat{x}, t^*)$ where t^* is defined by the condition

$$x_{f\pi} = \Phi_1(\hat{x}, t^*)_\pi = 0 \tag{3.28}$$

Now for the case of the ZDM, we had $t^* = \delta - \Delta$, although it is not clear that the final x_f lay in any linear transverse Poincaré section containing εx_0.

As with the ZDM we shall concentrate on terms up to $O(\varepsilon^{\frac{3}{2}})$ only. To that end, let us define

$$t^* = \tau_1 \varepsilon^{\frac{1}{2}} + \tau_2 \varepsilon + \tau_3 \varepsilon^{\frac{3}{2}} + O(\varepsilon^2).$$

Then, using the fact that

$$x_f = \Phi_1(\hat{x}, t^*) = \hat{x} + F_1 t^* + a_1 (t^*)^2 + b_1 \hat{x} t^* + c_1 (t^*)^3 + d_1 \hat{x}^2 t^* + e_1 \hat{x} (t^*)^2 + O(4), \tag{3.29}$$

from the Taylor expansion of (3.28) about the grazing point we have:

$$\begin{aligned}
0 &= \left(\hat{x} + F_1 t^* + a_1 (t^*)^2 + b_1 \hat{x} t^*\right)_\pi + O(3) \\
&= \left(\bar{x} + F_2 \Delta + a_2 \Delta^2 + b_2 \bar{x} \Delta + F_1(\tau_1 \varepsilon^{\frac{1}{2}} + \tau_2 \varepsilon) + [a_1 \tau_1^2 + b_1(\bar{x} + F_2 \Delta)\tau_1]\varepsilon\right)_\pi + O(3) \\
&= \Bigg([-F_1\gamma_1 + F_2\nu_1 + F_1\tau_1]\varepsilon^{\frac{1}{2}} + [\chi_2 + F_2\nu_2 + F_1\tau_2 + a_2\nu_1^2 - b_2 F_1 \gamma_1 \nu_1 + a_1\tau_1^2 \\
&\quad + b_1\tau_1(F_2\nu_1 - F_1\gamma_1)]\Bigg)_\pi \epsilon + O(\varepsilon^{\frac{3}{2}})
\end{aligned} \tag{3.30}$$

Now it is possible to solve the above equation term by term to get an expression for τ_0, τ_1 etc. First, taking the $O(\varepsilon^{\frac{1}{2}})$ term we get

$$\tau_1 = \gamma_1 - \frac{F_{2\pi}}{F_{1\pi}} \nu_1 \tag{3.31}$$

which is well defined and non-zero since $F_{1\pi}$ and $F_{2\pi}$ are nonzero by (3.27). Notice that in the case where $F_{1\pi} = F_{2\pi} = 1$, which would be the case for an non-autonomous system where $\boldsymbol{\pi}$ is in the direction of t, then this expression for τ_1 reduces to the leading order expression for $\delta - \Delta$ and one recovers the leading order expression for the ZDM. More generally we have, after substituting (3.31) into (3.29),

$$\begin{aligned}
x_f &= \hat{x} + F_1 t^* + O(\varepsilon) = \left(-F_1\gamma_1 + F_2\nu_1 + F_1\gamma_1 - \frac{F_{2\pi}}{F_{1\pi}} F_1 \nu_1\right) \varepsilon^{\frac{1}{2}} + O(\varepsilon) \\
&= \nu_1 \left(F_2 - \frac{F_{2\pi}}{F_{1\pi}} F_1\right) \varepsilon^{\frac{1}{2}} + O(\varepsilon)
\end{aligned} \tag{3.32}$$

which is $O(\varepsilon^{\frac{1}{2}})$ unless

$$F_2 F_{1\pi} = F_1 F_{2\pi}. \tag{3.33}$$

Now this condition is satisfied precisely when F_2 is a scalar multiple of F_1. The scalar is $F_{2\pi}/F_{1\pi}$ which for non-autonomous systems with $\boldsymbol{\pi}$ chosen in the direction t must be 1. Thus for the ZDM the condition (3.33) reduces to $F_1 = F_2$ so that the condition for square root behaviour is $F_1 \neq F_2$. But more generally

we have shown that this term vanishes if $F_1 = KF_2$ for some constant K. Note that in the case of non-autonomous systems, this would imply a rescaling of the time variable ($\dot{t} = 1$) across the boundary. Thus, this is consistent with what was previously observed for the ZDM.

Now let us consider the case when (3.33) is satisfied and the $O(\varepsilon^{\frac{1}{2}})$ term vanishes. Now we need to calculate τ_2. From (3.30) we obtain

$$-F_{1\pi}\tau_2 = \chi_{2\pi} + F_{2\pi}\nu_2 + a_{2\pi}\nu_1^2 - (b_2F_1)_\pi\gamma_1\nu_1 + a_{1\pi}\tau_1^2 + (b_1F_2)_\pi\nu_1\tau_1 - (b_1F_1)_\pi\gamma_1\tau_1.$$

However, using the definition of χ_2, the first term on the right-hand side is

$$x_{0\pi} - F_{1\pi}\gamma_2 + a_{1\pi}\gamma_1^2 = -F_{1\pi}\gamma_2 + a_{1\pi}\gamma_1^2,$$

since $x_0 \in \Pi$. Hence

$$\tau_2 = \gamma_2 - \frac{1}{F_{1\pi}}\left(a_{1\pi}\gamma_1^2 + F_{2\pi}\nu_2 + a_{2\pi}\nu_1^2 - (b_2F_1)_\pi\gamma_1\nu_1 + a_{1\pi}\tau_1^2 + (b_1F_2)_\pi\nu_1\tau_1 - (b_1F_1)_\pi\gamma_1\tau_1\right). \tag{3.34}$$

First consider the case where $F_1 = F_2$. Then

$$\nu_1 = 2\gamma_1, \quad \tau_1 = \gamma_1 - \nu_1 = -\gamma_1, \quad b_iF_j = 2a_i,$$

which when substituted into (3.34) gives

$$\begin{aligned}\tau_2 &= (\gamma_2 - \nu_2) + \frac{a_{1\pi}}{F_{1\pi}}\left(-\gamma_1^2 - \gamma_1^2 + 4\gamma_1^2 - 2\gamma_1^2\right) + \frac{a_{2\pi}}{F_{1\pi}}\left(-4\gamma_1^2 + 4\gamma_1^2\right)\\ &= \gamma_2 - \nu_2.\end{aligned}$$

Hence in this case

$$t^* = (\gamma_1 - \nu_1)\varepsilon^{\frac{1}{2}} + (\gamma_2 - \nu_2)\varepsilon + O(\varepsilon^{\frac{3}{2}}) = \Delta - \delta + O(\varepsilon^{\frac{3}{2}}),$$

which is the same time as that defining x_f in the previous subsection. Therefore the $O(\varepsilon)$ term of x_f is the same as that for the ZDM which is the identity εx_0. Hence provided it is non-zero, the leading-order term in this case is $O(\varepsilon^{\frac{3}{2}})$. Specifically, this term is derived (using Maple) as:

$$\begin{aligned}\Xi_{PDM} &= \left[8c_2 - c_1 + (e_1 - 4e_2)F_1 + (2d_2 - d_1)F_1^2\right]\gamma_1^3\\ &\quad + \left[2(a_2 - a_1)\nu_2 + (2b_2 - b_1)\chi_2\right]\gamma_1 + F_1\tau_3 + \chi_3 + F_1\nu_3\end{aligned}$$

where

$$\begin{aligned}\tau_3 &= -\nu_3 - \frac{1}{F_{1\pi}}\{\left[8c_2 - c_1 + (e_1 - 4e_2)F_1 + (2d_2 - d_1)F_1^2 + 2(b_2 - b_1)a_1\right]_\pi\gamma_1^3\\ &\quad + \left[2(a_2 - a_1)\nu_2 - 2(a_2 - a_1)\gamma_2 + (2b_2 - b_1)x_0\right]_\pi\gamma_1 + \chi_{3\pi}\}.\end{aligned}$$

An expression for this term purely in terms of F_1, F_2 and their derivative can be found in Appendix 1, from where it can be seen that, like for the PDM, (3.35) is generically nonzero if $F_1 = F_2$ but either the first or second derivatives of F do not coincide across the boundary.

Finally, we are left with the case $F_1 = KF_2$, i.e. $F_{1\pi}/F_{2\pi} = K$ in (3.33). Then

$$\nu_1 = 2K\gamma_1, \quad \tau_1 = \gamma_1 - \frac{F_{2\pi}}{F_{1\pi}}\nu_1 = -\gamma_1, \quad b_1F_2 = \frac{2}{K}a_1, \quad b_2F_1 = 2Ka_2,$$

which substituted in (3.34) yields:

$$\begin{aligned}\tau_2 &= \gamma_2 - \frac{1}{F_{1\pi}}\left(a_{1\pi}\gamma_1^2 + F_{2\pi}\nu_2 + 4a_{2\pi}K^2\gamma_1^2 - 4a_{2\pi}\gamma_1^2 + a_{1\pi}\gamma_1^2 - 4a_{1\pi}\gamma_1^2 + 2a_{1\pi}\gamma_1^2\right)\\ &= \gamma_2 - \frac{1}{K}\nu_2 - \frac{a_{1\pi}}{F_{1\pi}}\left(\gamma_1^2 + \gamma_1^2 - 4\gamma_1^2 + 2\gamma_1^2\right) - \frac{a_{2\pi}}{F_{1\pi}}(4K^2\gamma_1^2 - 4K^2\gamma_1^2)\\ &= \gamma_2 - \frac{1}{K}\nu_2.\end{aligned}$$

Thus, in this case

$$t^* = (\gamma_1 - \nu_1)\varepsilon^{\frac{1}{2}} + (\gamma_2 - \frac{\nu_2}{K})\varepsilon + O(\varepsilon^{\frac{3}{2}}). \tag{3.35}$$

Substituting (3.35) into (3.29), we then get

$$\begin{aligned} x_f &= (\chi_1 + F_2\nu_1 + F_1\gamma_2)\,\varepsilon^{\frac{1}{2}} + \Big[x_0 - F_1\gamma_2 + 2a_1\gamma_1^2 + 4a_2K^2\gamma_1^2 + \frac{F_1\nu_2}{K} + \\ &\quad - b_1F_1\gamma_1^2 + F_1\left(\gamma_2 - \frac{\nu_2}{K}\right) - 2b_2F_1\gamma_1^2K\Big]\,\varepsilon + O(\varepsilon^{\frac{3}{2}}) = \varepsilon x_0 + O(\varepsilon^{\frac{3}{2}}). \end{aligned}$$

Thus, even in this case the $O(\varepsilon)$ term of x_f is the same as that for the ZDM which is the identity εx_0. Hence, the leading order term is also $O(\varepsilon^{\frac{3}{2}})$ which can be shown to be non-zero using computer-assisted algebraic manipulation. Moreover this should be no surprise because setting $F_1 = KF_2$ gives the same phase portrait as $F_1 = F_2$, just rescaling time in the region S^-. Hence the $O(\epsilon^{\frac{3}{2}})$ term is just a transformation under this rescaling of the term (3.35) and is therefore nonzero. In particular, if we define $\bar{F}_2 = KF_2$ then the formulae for case $F_1 = F_2$ apply with appropriate redefinition of the various constants a_2, b_2, c_2, etc.

4 Poincaré maps close to periodic orbits that graze

Now let us suppose that the system (1.1) depends smoothly on a parameter μ, and that at $\mu = 0$ there is a periodic orbit $x(t) = p(t)$ that grazes at the point $x = 0 = p(0)$ (where the phase of p has been fixed without loss of generality). Moreover we shall assume that this orbit is hyperbolic and hence isolated. Finally, we assume that there are no points of grazing along $p(t)$ other than at $t = 0$. Since these are both open conditions, then we also assume that they are true for a sufficiently small neighbourhood of $\mu = 0$ and $p(t)$.

Consider first the case of a non-autonomous system whose coefficients are periodic with period T. We are thinking here of the case of a forced oscillator system, for example. Then suppose that $p(t)$ is an mT-periodic orbit for some $m > 0$. Hence, for $\mu = 0$, $x = 0$ will be a fixed point of the time-mT flow map Π_{per} defined, in a full neighbourhood of $x = 0$, by solving the flow in a neighbourhood of $p(t)$ as if the switching manifold S were not present and ϕ_1 applied throughout the phase space. The assumptions on smooth parameter dependence, hyperbolicity and lack of further grazing then imply generically that

$$\Pi_{per} : x \mapsto Nx + M\mu + o(|x|, \mu), \tag{4.1}$$

for some nonsingular $n \times n$ matrix N and non-zero n-dimensional vector M. For simplicity, we assume the ZDM (3.26) to be μ-independent without loss of generality, since one can perform a local parameter-dependent change of co-ordinates if necessary.

A global time-mT map can be obtained by composing the ZDM with Π_{per}. If the vector field is discontinuous at the grazing point, the resulting global map can be written using (3.23) as

$$\Pi_{per} \circ \Pi_{ZDM} : \quad x \to \begin{cases} Nx + M\mu + o(|x|, \mu) & \text{if } \langle \nabla H, x\rangle > 0, \\ N\mathbf{w}\sqrt{|\langle \nabla H, x\rangle|} + M\mu + o(|x|, \mu) & \text{if } \langle \nabla H, x\rangle < 0. \end{cases} \tag{4.2}$$

If the vector field is continuous at the grazing point, the global map can instead be written as:

$$\Pi_{per} \circ \Pi_{ZDM} : \quad x \to \begin{cases} Nx + M\mu + o(|x|, \mu) & \text{if } \langle \nabla H, x\rangle > 0, \\ N\Big[x + \mathbf{v}_1(|\langle \nabla H, x\rangle|)^{\frac{3}{2}} + V_2x(|\langle \nabla H, x\rangle|)^{\frac{1}{2}} & \\ \quad + \mathbf{v}_3\langle \nabla H, \frac{\partial F_2}{\partial x}x\rangle(|\langle \nabla H, x\rangle|)^{\frac{1}{2}}\Big] + M\mu + o(|x|^2, \mu) & \text{if } \langle \nabla H, x\rangle < 0, \end{cases} \tag{4.3}$$

where $\mathbf{w}$, $\mathbf{v_1}$,V_2 and $\mathbf{v}_3$ can be derived from (3.26) and are listed in Sec. 2.2. Either of these maps then describes all trajectories that remain within a neighbourhood of the grazing orbit; a fixed point represents an mT-periodic orbit of the flow, period-n points represent mnT-periodic orbits, etc.

Now let us consider the more general case of an autonomous system, or a non-autonomous system with time taken to be one of the dynamical states. Here we shall use the Poincaré section Π defined in the previous

section. Now we have no need for information on the period of the hyperbolic periodic orbit $p(t)$, just that it represents the fixed point of a Poincaré map from Π to itself defined by the flow where ϕ_1 applies everywhere. The assumptions about hyperbolicity and no other grazings along $p(t)$ mean that this Poincaré map again takes the form (4.1) but where now the $\boldsymbol{\pi}$ component of Nx and M are irrelevant so as the map is really reduced to an $(n-1)$-dimensional one. For convenience of notation we shall continue to bear this in mind, but continue to stick to n-dimensional vectors. In order to account for the correction owing to the portions of trajectories that enter S^- in a neighbourhood of the grazing, we must compose Π with the PDM to obtain a global Poincaré map. Again, if $F_1 = F_2$ at grazing, this results in the map

$$\Pi_{per} \circ \Pi_{PDM} : \quad x \to \begin{cases} Nx + M\mu + o(|x|, \mu) & \text{if } \langle \nabla H, x \rangle > 0, \\ N\mathbf{w}_\pi \sqrt{|\langle \nabla H, x \rangle|} + M\mu + o(|x|, \mu) & \text{if } \langle \nabla H, x \rangle < 0, \end{cases} \tag{4.4}$$

where from (3.32), we get:

$$\mathbf{w}_\pi = 2(F_2 - \frac{F_{2\pi}}{F_{1\pi}} F_1) \frac{\langle \nabla H, \frac{\partial F_2}{\partial x} F_1 \rangle}{\langle \nabla H, \frac{\partial F_2}{\partial x} F_2 \rangle} \left(\frac{2}{\langle \nabla H, \frac{\partial F_1}{\partial x} F_1} \right)^{\frac{1}{2}}.$$

If the vector field is continuous at the grazing point, the global map can instead be written as:

$$\Pi_{per} \circ \Pi_{PDM} : \quad x \to \begin{cases} Nx + M\mu + o(|x|, \mu) & \text{if } \langle \nabla H, x \rangle > 0, \\ N \Big[x + \mathbf{v}_{1\pi} (|\langle \nabla H, x \rangle|)^{\frac{3}{2}} + V_{2\pi} x (|\langle \nabla H, x \rangle|)^{\frac{1}{2}} & \\ + \mathbf{v}_{3\pi} \langle \nabla H, \frac{\partial F_2}{\partial x} x \rangle (|\langle \nabla H, x \rangle|)^{\frac{1}{2}} \Big] + M\mu + o(|x|^2, \mu) & \langle \nabla H, x \rangle < 0, \end{cases} \tag{4.5}$$

where, from Appendix 1, we obtain:

$$\begin{aligned} \mathbf{v}_{1\pi} &= \mathbf{v}_1 - \frac{F_1}{F_{1\pi}} \Big\{ \frac{2}{3}(d_2 - d_1)F^2 + 2(b_2 a_1) - \frac{2}{3}\left[(b_1 a_1) + 2(b_2 a_2)\right] \\ &\quad - \frac{2}{a_{2H}}(a_{2\pi} - a_{1\pi}) \cdot \left[4c_{2H} + (b_2 a_1 - 2b_2 a_2)_H + (d_2 F^2)_H \right] \Big\}_\pi, \\ V_{2\pi} &= \mathbf{v_2} - \frac{F_1}{F_{1\pi}} \left[(b_2 - b_1) x_0 \right]_\pi, \\ \mathbf{v}_{3\pi} &= \mathbf{v}_3 + \frac{2}{a_{2H}} \frac{F_1}{F_{1\pi}} (a_{2\pi} - a_{1\pi}). \end{aligned}$$

These maps have the same general form as (4.2) and (4.3) but are defined from the $(n-1)$ dimensional Poincaré section Π to itself.

5 Examples 1: bilinear oscillators

To test the local theory derived in the previous section, we shall use it to perform the local analysis of grazings in the so-called bilinear oscillator defined by the equation [Shaw & Holmes 1983*b*]:

$$\ddot{x} + \zeta_i \dot{x} + k_i^2 x = \beta_i \cos(\omega t) \tag{5.1}$$

where $i = 1$ if $x > 0$ and $i = 2$ if $x < 0$.

Firstly, we set $x_3 := \omega t$ as an extra state defined by the equation $\dot{x}_3 = \omega$. We can then recast (5.1) as a set of first-order autonomous differential equations as:

$$\dot{x} = \begin{cases} A_1 x + B_1, & \text{if } H(x) = Cx > 0 \\ A_2 x + B_2, & \text{if } H(x) = Cx < 0 \end{cases}$$

where

$$\begin{aligned} A_1 &= \begin{pmatrix} 0 & 1 & 0 \\ -k_1^2 & -\zeta_1 & 0 \\ 0 & 0 & 0 \end{pmatrix}, \quad A_2 = \begin{pmatrix} 0 & 1 & 0 \\ -k_2^2 & -\zeta_2 & 0 \\ 0 & 0 & 0 \end{pmatrix}, \\ B_1 &= \begin{pmatrix} 0 \\ \beta_1 \cos x_3 \\ \omega \end{pmatrix}, \quad B_2 = \begin{pmatrix} 0 \\ \beta_2 \cos x_3 \\ \omega \end{pmatrix}, \\ C &= (1 \quad 0 \quad 0). \end{aligned} \tag{5.2}$$

Note that in this case, we have:

$$\left.\frac{\partial F_i}{\partial x}\right|_{x=0} = A_i, \qquad F_i|_{x=0} = \begin{pmatrix} 0 \\ \beta_i \\ \omega \end{pmatrix},$$

and the switching manifold is the set:

$$S = \{x \in R^2 : Cx = 0\}.$$

According to the local analysis presented above, the local behaviour exhibited by the bilinear oscillator about the grazing will vary according to the properties of the system vector field at the grazing point $x = 0$. Specifically, we should be expecting a $\sqrt{\epsilon}$ local behaviour if the vector field is discontinuous at the grazing point and an $\varepsilon^{\frac{3}{2}}$ behaviour otherwise. To test this hypothesis, we now proceed by computing the ZDM for the system under investigation in the two cases when the vector field is continuous and discontinuous at the grazing point.

5.1 Case 1: changing the damping or the stiffness term

We now seek to investigate the dynamics of the bilinear oscillator when the damping coefficient, ζ_i or the stiffness coefficients, k_i, change across the switching manifold, while the forcing remain the same. In this case, we set $\beta_1 = \beta_2 = \beta$ in (5.2) and, using the analysis presented above (cfr. eqs.(3.5),(3.9), (3.13),(3.22)), we get for the ZDM:

$$x_f = \varepsilon x_0 + \begin{pmatrix} \frac{2}{3}(\zeta_2 - \zeta_1)\gamma_1^3 \\ \left[\frac{2}{3}\left(\zeta_1^2 - \zeta_1\zeta_2\right) + \frac{1}{3}(k_1^2 - k_2^2)\right]\beta\gamma_1^3 + 2(k_1^2 - k_2^2)x_{10}\gamma_1 \\ 0 \end{pmatrix} \varepsilon^{\frac{3}{2}} + \dots$$

where $\varepsilon \in R$, $x_0 = (x_{10}\ x_{20}\ x_{30})^T$ and $\gamma_1 = \sqrt{2\frac{x_{10}}{\beta}}$. Hence, as expected, since in this case the vector field is still continuous across the boundary both the linear and quadratic term in (3.22) disappear and an $\varepsilon^{3/2}$ behaviour is predicted by the local theory.

As shown in Figs. 5(a) and 5(b), this analytical result is in perfect agreement with numerical simulations of the system. These numerical results were obtained by taking a pair of Poincaré sections Σ_1 and Σ_2 as in Fig. 3, sufficiently close to the grazing instant. The perturbation ε was applied on Σ_1 so that trajectories with $\varepsilon > 0$ cross S. The difference was then plotted on Σ_2 between the trajectory computed using system 1 alone and that computed using the true computations of system 1 and 2.

5.2 Case 2: Discontinuous vector field

To test the method further, we shall next investigate the local dynamics of the bilinear oscillator when the amplitude of the forcing term is varied between two different values across the switching manifold, i.e. $\beta_1 \neq \beta_2$ while $k_1 = k_2 = k$, $\zeta_1 = \zeta_2 = \zeta$ in (5.2). In this case, the bilinear oscillator is characterized by a

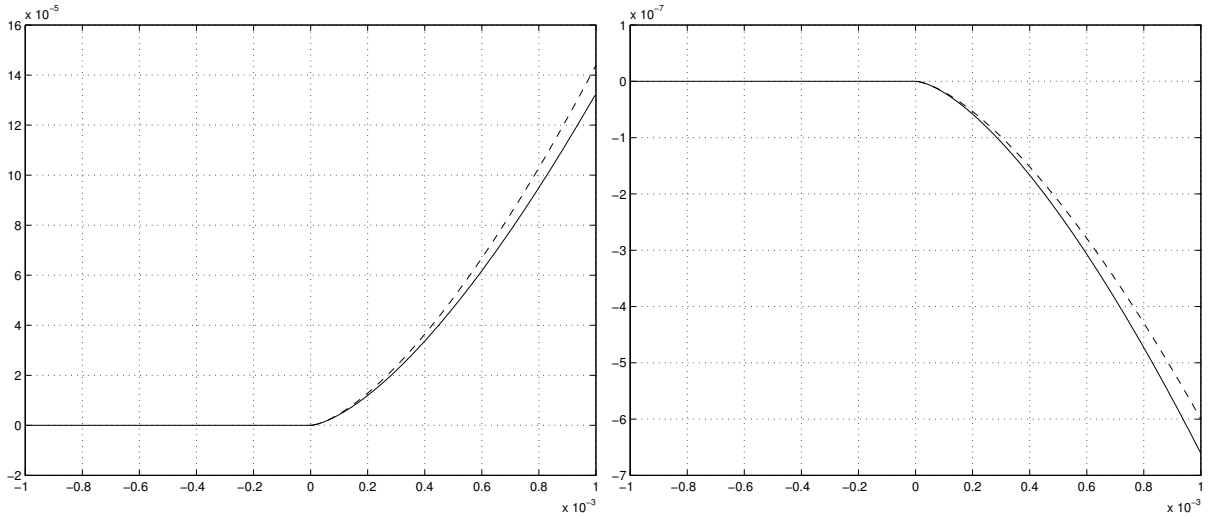

(a) **(b)**

Figure 5: Theoretical prediction (dashed line) and numerical simulation (solid line) of the local behaviour of the bilinear oscillator near grazing, when (a) the stiffness term, or (b) the damping term, is varied across S. In both $x_f - \varepsilon x_0$ is plotted against ε. Grazing occurs at $\varepsilon = 0$. The parameters in (5.1) are set to be (a) $k_1 = 1$, $k_2 = 2$, $\zeta_1 = \zeta_2 = 0.1$, $\beta_1 = \beta_2 = 1$ and (b) $k_1 = k_2 = 1$, $\zeta_1 = 0.1$, $\zeta_2 = 0.2$, $\beta_1 = \beta_2 = 1$.

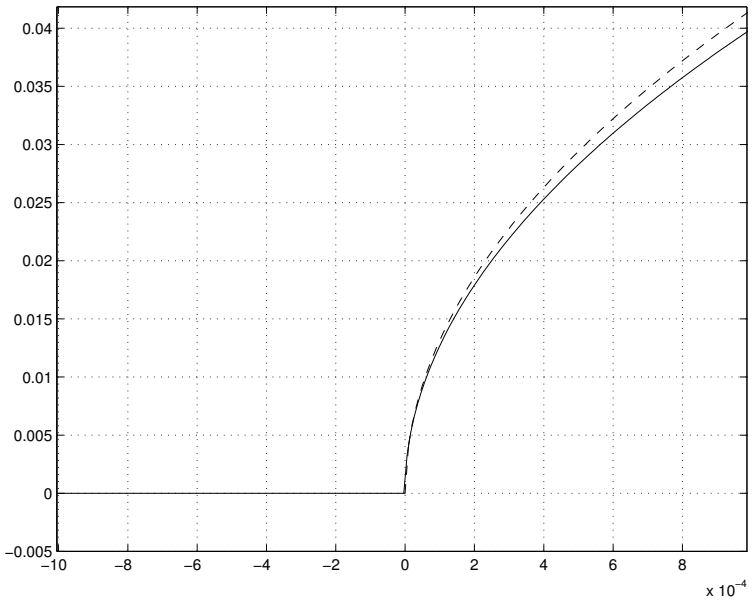

Figure 6: Local behaviour of the bilinear oscillator near grazing, when the forcing term is switched across S. $x_f - \varepsilon x_0$ is plotted against ε. Grazing occurs for $\varepsilon = 0$. The parameters in (5.1) are set to be $k_1 = k_2 = 1, \zeta_1 = \zeta_2 = 0.1, \beta_1 = 1, = \beta_2 = 2$

discontinuous vector field at the grazing point (i.e., $B_1 \neq B_2$) and the local analysis presented in Sec. 3.3.2 yields to lowest order:

$$x_f = \begin{pmatrix} 0 \\ -2\frac{\beta_1^2 - \beta_1\beta_2}{\beta_2}\gamma_1 \\ 0 \end{pmatrix} \varepsilon^{\frac{1}{2}} + \dots \tag{5.3}$$

Thus, as expected, we now have a $\varepsilon^{1/2}$ scaling law for the velocity perturbation. Note that for this to be true we need $\beta_1 \neq 0$ and $\beta_2 \neq 0$ and this is guaranteed by the grazing condition (2.6). As shown in Fig. 6, this is again confirmed by the numerical results.

6 Examples 2: Higher order systems

6.1 A third-order oscillator

We now consider a third-order oscillator described by the equation

$$\frac{d^3y}{dt^3} = -a_{3i}\frac{d^2y}{dt^2} - a_{2i}\frac{dy}{dt} - a_{1i}y + \beta_i \cos(\omega t). \tag{6.1}$$

This is a non-autonomous system and thus, as mentioned above, we would need to consider time as an extra state variable. The analysis of the previous section shows that in effect we can for small times treat this as an autonomous system. Specifically, for $t \ll 1$, $cos(\omega t) \approx 1$ and hence (6.1) can be recast as a system of first-order differential equations of the form

$$\dot{x} = \begin{cases} A_1 x + B_1, & \text{if } H(x) = Cx > 0 \\ A_2 x + B_2, & \text{if } H(x) = Cx < 0 \end{cases} \tag{6.2}$$

where

$$A_i = \begin{pmatrix} 0 & 1 & 0 \\ 0 & 0 & 1 \\ -a_{1i} & -a_{2i} & -a_{3i} \end{pmatrix}, B_i = \begin{pmatrix} 0 \\ 0 \\ \beta_i \end{pmatrix}, C = \begin{pmatrix} 1 \\ 0 \\ 0 \end{pmatrix}^T.$$

Note that this system can also be used to describe the dynamics of so-called relay feedback systems often used in control applications [Tsypkin 1984].

Firstly, we notice that, when $x = 0$, system (6.2) is such that:

1. $H(x) = Cx = 0$ for $x = 0$
2. $\nabla H(0,0) = C \neq 0$
3. $\langle \nabla H, F_i(0,0) \rangle = CB_i = 0$
4. $\frac{\partial H}{\partial x}\frac{\partial F_i}{\partial x}F_i = CA_iB_i = 0.$

Hence, the system does not satisfy all the conditions (2.3)–(2.5), (2.12) and (2.13) required for a grazing to occur at $x = 0$; specifically it violates the condition (2.12) on the curvature of the vector fields.

In fact, at the grazing point we have $x_1 = y = 0$, $x_2 = \dot{y} = 0$ and solving (6.1) we get:

$$x_3 = \ddot{y} = -\beta_i/a_{3i}.$$

Thus, for the oscillator described by (6.1), the grazing point is located at $x^* = (0, 0, -\beta_1/a_{31})$.

In order to apply the local theory we have presented above we need therefore to consider an appropriate change of coordinates to shift the grazing point from $x = x^*$ to $x = 0$ as required. Specifically, let $z = x - x^*$ so that system (6.2) becomes

$$\dot{z} = \begin{cases} A_1 z + B_1, & \text{if } Cz > 0 \\ A_2 z + B_2, & \text{if } Cz < 0 \end{cases} \tag{6.3}$$

where, in this case:

$$A_i = \begin{pmatrix} 0 & 1 & 0 \\ 0 & 0 & 1 \\ -a_{1i} & -a_{2i} & -a_{3i} \end{pmatrix}, B_1 = \begin{pmatrix} 0 \\ \lambda \\ a_{31}\lambda + \beta_1 \end{pmatrix}, B_2 = \begin{pmatrix} 0 \\ \lambda \\ a_{32}\lambda + \beta_2 \end{pmatrix}, C = \begin{pmatrix} 1 \\ 0 \\ 0 \end{pmatrix}^T. \tag{6.4}$$

with $\lambda = -\beta_1/a_{31}$. Note that system (6.3) satisfies all the properties required for a grazing to occur at $z = 0$. Thus, according to the local theory derived in the previous section, we will observe a $\varepsilon^{1/2}$ behaviour if the vector field is discontinuous i.e.:

$$B_1 \neq B_2.$$

From (6.4), we can deduce that this is verified if and only if $a_{31} \neq a_{32}$ or $\mu_1 \neq \mu_2$, i.e. if the amplitude of the forcing term or the coefficient of $\ddot{y}$ varies across S. For all other cases, $B_1 = B_2$ and a $\varepsilon^{3/2}$ local behaviour should instead be expected.

In fact, assuming $a_{31} \neq a_{32}$ while $a_{11} = a_{12}, a_{21} = a_{22}, \beta_1 = \beta_2$ in (6.4) we get from (3.22)

$$x_f = \begin{pmatrix} 0 \\ 0 \\ 2\left[\lambda(a_{32} - a_{31}) + (\beta_2 - \beta_1)\right]\gamma_1 \end{pmatrix} \varepsilon^{\frac{1}{2}} + \dots$$

Thus the third component of the state perturbation exhibits $\varepsilon^{\frac{1}{2}}$ behaviour as expected.

If, instead, we assume $a_{31} = a_{32} = \alpha$, $\beta_1 = \beta_2 = \beta$ but suppose that $a_{11} \neq a_{12}, a_{21} \neq a_{22}$, then the ZDM analysis yields:

$$x_f = \varepsilon x_0 + \begin{pmatrix} 0 \\ \frac{2}{3}(a_{21} - a_{22})\gamma_1^3 \\ \frac{1}{3}\left[a_{11} - a_{12} + 2\alpha(a_{21} - a_{22})\right]\lambda\gamma_1^3 + 2(a_{11} - a_{12})x_{10}\gamma_1 \end{pmatrix} \varepsilon^{\frac{3}{2}} + \dots$$

Hence, in this case, we have a $\varepsilon^{3/2}$ variation as anticipated by the theory.

6.2 A general third-order system

We next consider the case of a more general third-order system of the form

$$\dot{x} = \begin{cases} A_1 x + B_1, & \text{if } H(x) = Cx > 0 \\ A_2 x + B_2, & \text{if } H(x) = Cx < 0 \end{cases} \tag{6.5}$$

where

$$A_i = \begin{pmatrix} 0 & 1 & 0 \\ q_{1i} & q_{2i} & q_{3i} \\ r_{1i} & r_{2i} & r_{3i} \end{pmatrix}, B_i = \begin{pmatrix} \beta_{1i} \\ \beta_{2i} \\ \beta_{3i} \end{pmatrix}, C = \begin{pmatrix} 1 \\ 0 \\ 0 \end{pmatrix}^T. \tag{6.6}$$

Following the same approach outlined above, the ZDM is derived to be

$$x_f = \begin{pmatrix} 2\gamma_1 \frac{\beta_{21}}{\beta_{22}}(\beta_{11} - \beta_{12}) \\ 2\gamma_1 \frac{\beta_{21}}{\beta_{22}}(\beta_{21} - \beta_{22}) \\ -2\gamma_1 \frac{\beta_{21}}{\beta_{22}}(\beta_{31} - \beta_{32}) \end{pmatrix} \varepsilon^{\frac{1}{2}} + O(\varepsilon) \tag{6.7}$$

Note that if $\beta_{22} = 0$ then there is no contradiction suggested by the formula (6.7) because in this case CA_2B_2 would be equal to zero, thus breaking the assumption that the system has a grazing at $x = 0$. Also note that we must have $\beta_{21} \neq 0$ by the definition of grazing, otherwise condition (2.6) is violated.

This example is similar to that of a second-order oscillator in that grazing occurs when the first component of x (the 'position') passes through zero, with the second component of x acting like velocity. However, note that the vector field may be continuous in these two variables ($\beta_{11} = \beta_{12}$ and $\beta_{21} = \beta_{22}$), yet if it is discontinuous in the third component ($\beta_{31} \neq \beta_{32}$) then we still see a non-zero square-root singularity.

Similarly to what was found in the previous example, the ZDM for a general third-order system such as (6.5) can also be shown to be $O(\varepsilon^{\frac{3}{2}})$ to leading order when $B_1 = B_2$.

6.3 An autonomous system

Finally, let us end with an example where we compute a PDM. Specifically we shall take a constructed example of an autonomous three-dimensional system which can be solved in closed form. Then we can compare the PDM calculated using the above theory with that calculated by solving the equations directly (up to implicit transcendental equations defining the *a priori* unknown times that a trajectory hits the switching manifold).

Consider a system defined by

$$\begin{array}{rcl} \dot{r} &=& \varepsilon_i r(a-r) \\ \dot{\theta} &=& \omega_i \\ \dot{z} &=& \beta_i z + \gamma_i \end{array} \quad , \quad (i=1,2) \quad \text{where} \quad x = r\cos\theta,\ y-1 = r\sin\theta, \tag{6.8}$$

where $i=1$ corresponds to $y>0$ and $i=2$ corresponds to $y<0$. Then the switching manifold is given by

$$S = \{(x,y,z)|\ y=0\}, \quad \text{and} \quad \nabla H = (0,1,0),$$

S^+ is the region $y>0$ and S^- is $y<0$, and a suitable choice of Poincaré section is

$$\Pi = \{(x,y,z)|\ x=0\}, \quad \text{so that} \quad \boldsymbol{\pi} = (1,0,0).$$

For simplicity we shall henceforth assume that $\omega_1 = 1$ and $\gamma_1 = 0$, $\varepsilon_1 > 0$ and $\beta_1 < 0$. Then, for $a=1$, by construction the system (6.8) possesses a limit cycle $r=1$, $\theta = t$ of period 2π which grazes with S. Moreover, as $a \to 1^-$ this solution is the limit of a continuous branch of stable 2π-periodic solution $r=a$ contained within region S^+. The linearization around this periodic orbit for $a=1$ evaluated on Π (ignoring the trivial direction along x) is given by

$$\begin{bmatrix} y \\ z \end{bmatrix} \mapsto N \begin{bmatrix} y \\ z \end{bmatrix}, \quad \text{where} \quad N = \begin{bmatrix} e^{-2\varepsilon_1\pi} & 0 \\ 0 & e^{-2\beta_1\pi} \end{bmatrix} \tag{6.9}$$

and the linearization with respect to the bifurcation parameter $\mu = (a-1)$ is

$$M = \begin{bmatrix} 1 - e^{-2\varepsilon_1\pi} \\ 0 \end{bmatrix}. \tag{6.10}$$

Note that an explicit solution can be found for any point in regions S^+ or S^- with initial conditions (r_0, θ_0, z_0):

$$\begin{array}{rcl} r(t) &=& \dfrac{a r_0}{r_0 + (a-r_0)e^{-a\varepsilon_i t}}, \\ \theta(t) &=& \theta_0 + \omega_i t, \\ z(t) &=& \dfrac{1}{\beta_i}\left((c-\beta_i z_0)e^{\beta_i t} - c\right). \end{array} \tag{6.11}$$

Let us stick to the case $a=1$. The exact Poincaré map for initial conditions on Π with $y>0$ is then just given by the solution of (6.11) with $i=1$ and $t=2\pi$. For initial conditions on Π with $y_0<0$, equations (6.11) can be solved in region S^- ($i=2$) until the implicitly defined time t_1 at which $y=0$. Next we solve in region S^+ until the next time t_2 at which $y=0$ whereupon we switch back to solving the system in S_- until t_3 which is the first subsequent time that $x=0$. This then defines an 'exact' Poincaré mapping. In fact, the times $t_{1,2,3}$ are defined by the solution of implicit equations, which we implement in Maple using accurate root-finding to find the first positive root in each case.

This exact map can be compared with the approximate map evaluated using the preceding analysis. In particular we find for the case that the vector field is discontinuous at the grazing point (assuming $c_1 = 1, \omega_1 = 1$):

$$\mathbf{w}_\pi = \left(0\ ,\ 2\sqrt{2}\,\frac{\gamma_2}{\omega_2}\right)^T.$$

Then, given the definition of N and M, which define the linearization of the global Poincaré map, according to (4.4) the PDM in this case is

$$\Pi_{per} \circ \Pi_{PDM} : \quad \begin{bmatrix} y \\ z \end{bmatrix} \mapsto \begin{bmatrix} 0 \\ \frac{2\sqrt{2}\,\gamma_2}{\omega_2} e^{-2b_1\pi}\sqrt{|y|} \end{bmatrix} + \mathcal{O}(y,z) \quad \text{for} \quad y < 0.$$

Note that it is similarly possible to define the topologically equivalent map $\Pi_{PDM} \circ \Pi_{per}$. Figure 7(a) compares both of these two global PDMs with the exact expression in each case plotting the z-component of the map as a function of the y-component of the initial condition. Note how the exact map lies exactly between $\Pi_{PDM} \circ \Pi_{per}$ and $\Pi_{per} \circ \Pi_{PDM}$ each of which clearly has a square-root behaviour.

This now raises a subtle point. The PDM in fact only describes something that is topologically equivalent to the leading-order expression for the true Poincaré map from $\Pi \to \Pi$. This is because the PDM as defined first makes a correction and then solves all the way around the trajectory using the flow 1. The alternative $\Pi_{per} \circ \Pi_{PDM}$ performs these two operations in reverse. Whereas the true flow makes only half of its passage through S^- to begin with, and half at the end. Perhaps a better method, to overcome this difficulty, is to work with a new Poincaré section Π_2 that is away from the grazing point. For the present example we could take Π_2 to be the local Poincaré section that is defined by Π in a neighbourhood of $(x, y, z) = (0, 2, 0)$. Then the linearization around the periodic orbit at the grazing point can be composed of two pieces

$$\Pi_{per} = \Pi^{(2)}_{per} \circ \Pi^{(1)}_{per}$$

where $\Pi^{(1)}_{per} : \Pi_2 \to \Pi$, and $\Pi^{(2)}_{per} : \Pi \to \Pi_2$. Then we can construct a global PDM from Π_2 to Π_2 via

$$\Pi^*_{PDM} = \Pi^{(2)}_{per} \circ \Pi_{PDM} \circ \Pi^{(1)}_{per}$$

In fact for (6.8) we have that $\Pi^{(1)}_{per} = \Pi^{(2)}_{per} = (\Pi_{per})^{\frac{1}{2}}$ and thus we obtain

$$\Pi^*_{PDM} : \quad \begin{bmatrix} y \\ z \end{bmatrix} \mapsto \begin{bmatrix} 0 \\ \frac{2\sqrt{2}\,\gamma_2}{\omega_2} e^{\beta_1 t\pi}\sqrt{|e^{-\varepsilon_1\pi} y|} \end{bmatrix} + \mathcal{O}(y,z) \quad \text{for} \quad y < 0. \tag{6.12}$$

Figure 7(b) shows the comparison between this map and the equivalent exact expression for the same map. The agreement is perfect.

Similar expressions can be derived for the case when the vector field is continuous at the grazing point. But for brevity we leave out such expressions here. Figure 7(b) shows the exact map in this case, showing how the y-component varies as a function of an initial perturbation in y. Figure 7(c) then shows the difference between this map and the map obtained by solving the flow as if the boundary were not there, together with an approximate fit to the data. Clearly we are seeing $\varepsilon^{3/2}$ behaviour precisely as predicted by the theory.

7 Conclusion

In this paper we have presented an effective method for the derivation of local maps to describe the dynamics of n-dimensional piecewise-smooth dynamical systems near grazing. Using asymptotics and formal power series expansions we have shown that discontinuities in the system vector field at the grazing point yield normal forms characterized by square root singularities. A (3/2)-type singularity is instead detected in maps associated with vector fields which are continuous at the grazing point.

Contrary to what has often been assumed in the literature (e.g. [Feigin 1970]), **our results rule out the possibility of piecewise linear normal forms** unless the switching manifold is itself non-smooth [di Bernardo, Budd & Champneys 2000*b*].

An interesting open problem is that of characterizing the local behaviour of PWS systems undergoing grazing bifurcations in regions were sliding motion is possible (i.e., when (2.9) is not satisfied — the situation depicted in Fig. 1(b)). In such cases, the dynamics are likely to be very different. Preliminary numerical results are

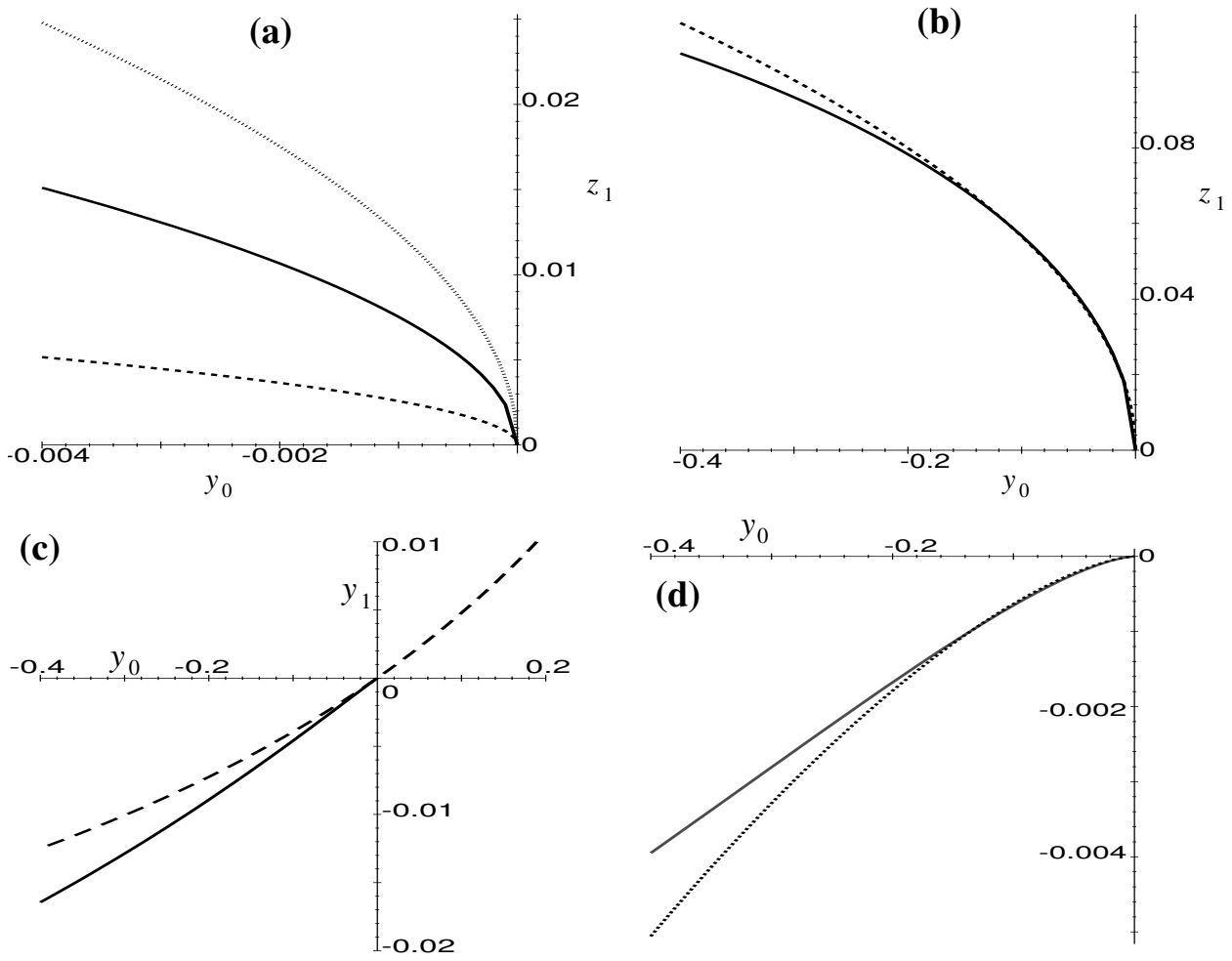

Figure 7: Agreement between the 'exact' Poincaré map calculated by solving the implicit equations and the 'calculated' PDM using the theory for the example (6.8) with $a = 1$, $\beta_1 = \varepsilon_1 = 1/2$, $\omega_1 = 1$, $\gamma_1 = 0$; and (a)–(b) $\beta_2 = \varepsilon_2 = 1/2$, $\gamma_2 = 1$ and $\omega = 3/2$; (c)–(d) $\beta_2 = \varepsilon_2 = 1/5$, $\gamma_2 = 0$ and $\omega = 0$. In (a), the final value of the z-coordinate is plotted against initial perturbation in $y < 0$ for the exact map (solid line), $\Pi_{per} \circ \Pi_{PDM}$ (dashed line) and $\Pi_{PDM} \circ \Pi_{per}$ (dotted line). (b) Then compares the exact map with Π^*_{PDM} defined by (6.12). (c) Shows, for a case with continuity of the vector field at the grazing, the exact expression for the Poincaré map (solid line) against the unperturbed map as if the boundary were not there (dashed line). Plotted is the final y-value against initial perturbation in y. Finally, (d) shows the difference between these two maps (solid line) together with the curve $-0.02\ {y_0}^{3/2}$ (dotted).

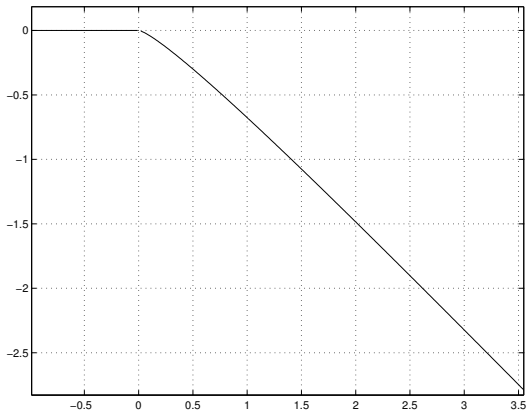

Figure 8: Global behaviour of a second-order bilinear oscillator when the damping coefficient is varied across the switching manifold. As with previous figures $x_f - \varepsilon x_0$ is plotted against ε. Despite the local (3/2) behaviour, a piecewise linear global behaviour can be observed.

reported in [di Bernardo, Johansson & Vasca 2000]. In particular it was demonstrated that novel bifurcations can occur which cause the transition to sliding and to so-called *multi-sliding* periodic solutions. A complete analysis is the subject of ongoing research.

It is worth mentioning here that our analysis is purely local and it captures only the dynamics associated with trajectories that are sufficiently close to the grazing one in both phase and parameter space. This is entirely equivalent to the situation for the analysis of local bifurcations of periodic orbits in smooth systems of ODEs. The power of this approach is that it allows the easy comparison of local maps associated with different vector fields and thus can be used as a general tools for the analysis of grazings in n-dimensional PWS systems.

An unsolved issue remains the *global* analysis of periodic orbits (or other attractors) in n-dimensional PWS systems away from a small neighbourhood of the grazing point. Preliminary results for a second-order oscillator are reported in Fig. 8. Here we see that the global map is piecewise linear to leading order even though the local map is $O(\varepsilon^{3/2})$. The derivation of a consistent theory explaining this global behaviour and its relationship to the local analysis reported in this paper is under investigation and will be reported elsewhere [di Bernardo, Budd & Champneys 2000*a*]. Undoubtedly, this will solve the problem, mentioned in the introduction, of studying analytically the convergence to square root behaviour of a bilinear oscillator characterized by an increasingly stiff wall.

Finally, in this paper we have not investigated the dynamics of the piecewise-smooth maps we have derived. Clearly in view of the literature reviewed in the introduction for piecewise-linear maps and the Nordmark map, the dynamics of our n-dimensional maps are likely to encompass a wide range of phenomena, including period-adding bifurcations and sudden jumps to chaos. These issues on the dynamical implications of our results will be the subject of future work.

Acknowledgements

We acknowledge a useful conversation with Arne Nordmark (RIT Stockholm), and also thank Harry Dankowicz of the same institution for comments on an earlier version. MdiB acknowledges support from the Nuffield Foundation (scheme 'NUF-NAL') and the International Center for Advanced Studies in Nizhny Novgorod (INCAS- project no. 99-1-02). ARC acknowledges the support of the UK EPSRC with whom he holds an Advanced Fellowship.

A Expressions for map coefficients

In what follows, we present the expressions for (3.26) and (3.35) written solely in terms of the vector field and its derivatives evaluated for the case of continuity at the grazing point, i.e. $F_1^0 = F_2^0 := F$. Specifically, from (3.26) we get

$$\Xi_{ZDM} = (\eta_1\gamma_1^3 + \eta_2\gamma_1 + \eta_3)\varepsilon^{\frac{3}{2}} \tag{A.1}$$

where

$$\begin{aligned} \eta_1 &= 8c_2 - c_1 + (e_1 - 4e_2)F + (2d_2 - d_1)F^2 && \text{(A.2)} \\ \eta_2 &= (2b_2 - b_1)\chi_2 + 2(a_2 - a_1)\nu_2, \\ \eta_3 &= \chi_3 + F\gamma_3. && \text{(A.3)} \end{aligned}$$

We observe now that $e_iF = d_iF^2 + b_ia_i$ and $c_i = \frac{1}{3}d_iF + \frac{1}{3}b_ia_i$, thus (A.2) yields:

$$\eta_1 = \frac{2}{3}d_2F^2 - \frac{1}{3}d_1F^2 - \frac{4}{3}b_2a_2 + \frac{2}{3}b_1a_1. \tag{A.4}$$

Moreover, using (3.9),(3.10), (3.6), (3.11), (3.14) and recalling that, if $F_1 = F_2 := F$, $\nu_1 = 2\gamma_1$, $b_iF_j = 2a_i$, we also get:

$$\eta_2 = \alpha_1\gamma_1^2 + \alpha_2 \tag{A.5}$$

where

$$\begin{aligned} \alpha_1 &= (2b_2 - b_1)(a_1 - \frac{c_{1H}}{2a_{1H}}F) - 2(a_2 - a_1)\Psi, \\ \alpha_2 &= (2b_2 - b_1)(x_0 - \frac{(b_1x_0)_H}{2a_{1H}}F) - 2(a_2 - a_1)\left[\frac{(b_2x_0)_H}{a_{2H}} - \frac{(b_1x0)_H}{a_{1H}}\right], \end{aligned}$$

and

$$\Psi = \frac{1}{a_{2H}}\left[(b_2a_1)_H - 2(b_2a_2)_H + 4c_{2H} - c_{1H} - (d_2F^2)_H\right]. \tag{A.6}$$

Finally, from (A.3), we get:

$$\eta_3 = \beta_1\gamma_1^3 + \beta_2\gamma_1 \tag{A.7}$$

where

$$\begin{aligned} \beta_1 &= \frac{a_1}{a_{1H}}c_{1H} - c_1, \\ \beta_2 &= \frac{a_1}{a_{1H}}(b_1x_0)_H - b_1x_0. \end{aligned}$$

Hence, (A.1) can be rewritten as:

$$\Xi_{ZDM} = (\zeta_1\gamma_1^3 + 2(b_2 - b_1)x_0\gamma_1 - 2(a_2 - a_1)\frac{(b_2x_0)_H}{a_{2H}}\gamma_1)\varepsilon^{\frac{3}{2}} \tag{A.8}$$

where

$$\begin{aligned} \zeta_1 &= \eta_1 + \alpha_1 + \beta_1 = \frac{2}{3}(d_2 - d_1)F^2 + 2b_2a_1 - \frac{2}{3}(b_1a_1 + 2b_2a_2) \\ &\quad -\frac{2}{a_{2H}}(a_2 - a_1)\left[4c_{2H} + (b_2a_1 - 2b_2a_2)_H + (d_2F^2)_H\right]. \end{aligned}$$

Therefore, using (3.5), we get :

$$\Xi_{ZDM} = \frac{1}{\sqrt{a_{1H}}}\left[\frac{\zeta_1}{a_{1H}}x_{0H}^{\frac{3}{2}} + 2(b_2 - b_1)x_0x_{0H}^{\frac{1}{2}} - \frac{2}{a_{2H}}(a_2 - a_1)(b_2x_0)_Hx_{0H}^{\frac{1}{2}}\right]\varepsilon^{\frac{3}{2}} \tag{A.9}$$

Note that if the vector field is supposed to be C^1, i.e. $F_1 = F_2$ and $\frac{\partial F_1}{\partial x} = \frac{\partial F_2}{\partial x}$ then $a_1 = a_2$, $b_1 = b_2$ and (A.8) becomes

$$\Xi_{ZDM} = \frac{2}{3} a_{1H}^{-\frac{3}{2}} (d_2 - d_1) F^2 (\varepsilon x_0)^{\frac{3}{2}} \tag{A.10}$$

Thus, from the definition of d_i in (2.15) we get that the $O(\varepsilon^{\frac{3}{2}})$ is still the leading order term in the ZDM if the vector field is continuous together with its first derivative but

$$\frac{\partial^2 F_1}{\partial x^2} \neq \frac{\partial^2 F_2}{\partial x^2}$$

By similar manipulations, it is possible to show from (3.35) that

$$\Xi_{PDM} = \Xi_{ZDM} + \eta_4 \varepsilon^{\frac{3}{2}} \tag{A.11}$$

where

$$\eta_4 = \frac{F_1}{F_{1\pi}} \left[\zeta_{1\pi} \gamma_1^3 + 2 \left[(b_2 - b_1) x_0 \right]_\pi \gamma_1 - \frac{2}{a_{2H}} (a_{2\pi} - a_{1\pi}) (b_2 x_0)_H \right]$$

with

$$\begin{aligned} \zeta_{1\pi} \;=\; & \frac{2}{3} \left[(d_2 - d_1) F^2 \right]_\pi + 2 (b_2 a_1)_\pi - \frac{2}{3} (b_1 a_1 + 2 b_2 a_2)_\pi \\ & - \frac{2}{a_{2H}} (a_{2\pi} - a_{1\pi}) \left[4 c_{2H} + (b_2 a_1 - 2 b_2 a_2)_H + (d_2 F^2)_H \right] \end{aligned}$$

Notice that, in this case, if the vector field is supposed to be C^1, i.e. $a_1 = a_2$, $b_1 = b_2$, (A.11) yields

$$\Xi_{PDM} = \frac{2}{3} a_{1H}^{-\frac{3}{2}} \left[(d_2 - d_1) F^2 - \frac{F}{F_\pi} \left[(d_2 - d_1) F^2 \right]_\pi \right] (\varepsilon x_0)^{\frac{3}{2}} \tag{A.12}$$

Thus, even in this case, the $O(\varepsilon^{\frac{3}{2}})$ is still the leading order term of the PDM if the vector field is continuous together with its first derivative but

$$\frac{\partial^2 F_1}{\partial x^2} \neq \frac{\partial^2 F_2}{\partial x^2}.$$

References

Babitskii, V. [1978], *Theory of Vibroimpact Systems. Approximate methods*, Nauka, Moscow.

Banerjee, S. & Grebogi, C. [1999], 'Border collision bifurcations in two-dimensional piecewise smooth maps', *Physical Review E* **59**, 4052–4061.

Brogliato, B. [1999], *Nonsmooth Mechanics*, Springer–Verlag.

Budd, C. & Dux, F. [1994*a*], 'Chattering and related behaviour in impact oscillators', *Phil. Trans. Royal Society London A* **347**, 365–389.

Budd, C. & Dux, F. [1994*b*], 'Intermittency in impact oscillators close to resonance', *Nonlinearity* **7**, 1191–1224.

Chin, W., Ott, E., Nusse, H. E. & Grebogi, C. [1994], 'Grazing bifurcations in impact oscillators', *Physical Review E* **50**, 4427–4444.

Dankowicz, H. & Nordmark, A. [1999], 'On the origin and bifurcations of stick-slip oscillations', *Physica D* **136**, 280–302.

Deane, J. & Hamill, D. [1990], Analysis, simulation and experimental study of chaos in the buck concerter, *in* 'Proceedings of the Power Electronics Specialists Conf. (PESC 1990)', IEEE Press, New York, pp. 491–8.

di Bernardo, M., Budd, C. & Champneys, A. [2000*a*], Global analysis of grazing in piecewise smooth dynamical systems, in preparation.

di Bernardo, M., Budd, C. & Champneys, A. R. [2000*b*], Corner–collision implies border–collision bifurcation, submitted to Physica D.

di Bernardo, M., Champneys, A. R. & Budd, C. J. [1998], 'Grazing, skipping and sliding: analysis of the nonsmooth dynamics of the DC/DC buck converter', *Nonlinearity* **11**, 858–890.

di Bernardo, M., Feigin, M., Hogan, S. & Homer, M. [1999], 'Local analysis of C-bifurcations in n-dimensional piecewise smooth dynamical systems', *Chaos, Solitons and Fractals* **10**, 1881–1908.

di Bernardo, M., Garofalo, F., Glielmo, L. & Vasca, F. [1998], 'Switchings, bifurcations and chaos in DC/DC converters', *IEEE Transactions on Circuits and Systems, Part I* **45**, 133–141.

di Bernardo, M., Johansson, K. & Vasca, F. [2000], Self-oscillations and sliding in relay feedback systems: Symmetry and bifurcations, to appear on International Journal of Bifurcations and Chaos.

Doole, S. H. & Hogan, S. J. [1996], 'A piecewise linear suspension bridge model: nonlinear dynamics and orbit continuation', *Dynamics and Stability of Systems* **11**, 19–29.

Feigin, M. I. [1970], 'Doubling of the oscillation period with c-bifurcations in piecewise continuous systems', *PMM* **34**, 861–869.

Feigin, M. I. [1974], 'On the generation of sets of subharmonic modes in a piecewise continuous system', *PMM* **38**, 810–818.

Feigin, M. I. [1978], 'On the structure of C-bifurcation boundaries of piecewise continuous systems', *PMM* **42**, 820–829.

Feigin, M. I. [1995], 'The increasingly complex structure of the bifurcation tree of a piecewise-smooth system', *Journal of Appl. Maths. Mechs* **59**, 853–863.

Feigin, M. I. [1996], 'Fundamental dynamic models and criteria of C-bifurcation structures for piecewise smooth systems', *Proceedings of the International Symposium on Analysis and Synthesis of Nonlinear Dynamical Systems* pp. 30–40. Riga, Latvia.

Filippov, A. [1988], *Differential equations with discontinuous righthand sides*, Kluwer, Dortrecht.

Foale, S. [1994], 'Analytical determination of bifurcations in an impact oscillator', *Phil. Trans. Roy. Soc. London A* **347**, 353–364.

Foale, S. & Bishop, S. R. [1994], 'Bifurcations in impact oscillators', *Nonlinear Dynamics* **6**, 285–299.

Fossas, E. & Olivar, G. [1996], 'Study of chaos in the buck converter', *IEEE Transactions on Circuits and Systems - I: Fundamental Theory and Applications* **43**, 13–25.

Frederiksson, M. & Nordmark, A. [1997], 'Bifuractions caused by grazing incidence in many degrees of freedom impact oscillators', *Proc. Royal Soc. London A* **453**, 1261–1276.

Frederiksson, M. & Nordmark, A. [2000], 'On normal form calculations in impact oscillators', *Proc. Royal Soc. London A* **456**, 315–329.

Hogan, S. J. [1989], 'On the dynamics of rigid-block motion under harmonic forcing', *Proc. Roy. Soc. London A* **425**, 441–476.

McGeer, T. [1990], 'Passive dynamic walking', *Int. Journal of Robotics Research* **9**, 62–82.

Nordmark, A. [1997], 'Universal limit mapping in grazing bifurcations', *Physical Review E* **55**, 266–270.

Nordmark, A. B. [1991], 'Non-periodic motion caused by grazing incidence in impact oscillators', *Journal of Sound and Vibration* **2**, 279–297.

Norsworthy, S. R., Schreier, R. & Temes, G. C. [1997], *Delta-Sigma Data Converters—Theory, Design, and Simulation*, IEEE Press, New York.

Nusse, L. E. & Yorke, J. A. [1992], 'Border-collision bifurcations including 'period two to period three' for piecewise smooth systems', *Physica D* **57**, 39–57.

Nusse, L. E. & Yorke, J. A. [1994], 'Border collision bifurcation: an explanation for observed bifurcation phenomena', *Physical Review E* **49**, 1073–1076.

Nusse, L. E. & Yorke, J. A. [1995], 'Border–collision bifurcations for piece-wise smooth one-dimensional maps', *International Journal of Bifurcation and Chaos* **5**, 189–207.

Peterka, F. [1974], 'Part 1: Theoretical analysis of n-multiple $(1/n)$-impact solutions', *CSAV Acta Technica* **26**(2), 462–473.

Popp, K., Hinrichs, N. & Oestreich, M. [1995], 'Dynamical behaviour of friction oscillators with simultaneous self and external excitation', *Sadhana (Indian Academy of Sciences)* **20**, 627–654.

Shaw, S. & Holmes, P. [1983*a*], 'Periodically forced linear oscillator with impacts: chaos and long-periodic motions', *Phys. Rev. Lett.* **51**, 623–626.

Shaw, S. & Holmes, P. [1983*b*], 'A periodically forced piecewise linear oscillator.', *J. Sound and Vibration* **90**, 129–144.

Thompson, J. & Ghaffari, R. [1983], 'Chaotic dynamics of an impact oscillator', *Phys. Rev. A* **27**, 1741–1743.

Tsypkin, Ya. Z. [1984], *Relay Control Systems*, Cambridge University Press, Cambridge, U.K.

Whiston, G. S. [1987], 'The vibro-impact response of a harmonically excited and preloaded one-dimensional linear oscillator', *Journal of Sound and Vibrations* **115**, 303–324.

Yuan, G., Banerjee, S., Ott, E. & Yorke, J. [1998], 'Border-collision bifurcations in the buck converter', *IEEE Transactions on Circuits and Systems–I* **45**, 707–716.